



Scientific Validation Report for iSHAI Product Processors of the NWC/GEO MTG-I Day-1

NWC/CDOP4/MTG/AEMET/SCI/VR/iSHAI, Issue 1, Rev.0.0

31 March 2025

Applicable to GEO-iSHAI v5.0 (NWC-033)

REPORT SIGNATURE TABLE

Function	Name	Signature	Date
Prepared by	Miguel A. Martinez (AEMET)		31 March 2025
Reviewed by	Xavier Calbet, AEMET (NWC SAF GEO Manager)		31 March 2025
Authorised by	Pilar Ripodas, AEMET (NWC SAF Project Managers)		31 March 2025

DOCUMENT CHANGE RECORD

Version	Date	Pages	CHANGE(S)
1.0.0	31 March 2025	57	Version for ORR2.

TABLE OF CONTENTS

1.	INTRODUCTION.....	9
1.1	<i>SCOPE OF THE DOCUMENT</i>	<i>9</i>
1.2	<i>SOFTWARE VERSION IDENTIFICATION.....</i>	<i>9</i>
1.3	<i>GLOSSARY</i>	<i>9</i>
1.4	<i>REFERENCES</i>	<i>11</i>
1.4.1	<i>NWC SAF Applicable Documents</i>	<i>11</i>
1.4.2	<i>Reference Documents</i>	<i>12</i>
2.	MTG-I1/FCI AND SEVIRI GEO-ISHAI VALIDATION DATASET.....	13
2.1	<i>DESCRIPTION OF FILES USED.....</i>	<i>13</i>
2.2	<i>DESCRIPTION OF PROCESS TO GENERATE THE VALIDATION DATASET</i>	<i>14</i>
3.	VALIDATION RESULTS.....	19
3.1	<i>2D DIMENSIONAL HISTOGRAMS OF GEO iSHAI PARAMETERS.....</i>	<i>19</i>
3.2	<i>SPATIAL ANALYSIS OF GEO iSHAI PARAMETERS.....</i>	<i>35</i>
3.3	<i>SUMMARY OF LPW AND STABILITY INDICES PERFORMANCES.....</i>	<i>46</i>
3.4	<i>ANALYSIS OF THE PERFORMANCE AT DIFFERENT VERTICAL LEVELS.....</i>	<i>46</i>
3.5	<i>VALIDATION OF GEO-iSHAI SKT: SKIN TEMPERATURE.....</i>	<i>52</i>
4.	CONCLUSIONS	56

List of Tables and Figures

Table 1: List of Applicable Documents.	12
Table 2: List of Referenced Documents.....	12
Figure 1: Predefined set of 13001 validation points used in validation datasets. Grid network of 1° x 1° plus Radiosonde Stations (red crosses).....	15
Figure 2: Generation of the records for adding to GEO iSHAI validation dataset from one image for (t+00), (t+12) and (t+24) cases for MTII/FCI and MSG3/SEVIRI	16
Figure 3: GEO iSHAI validation scheme.	18
Figure 4: BT_RTTOV FCI MTII case: LPW and TPW 2D histograms over sea validation points. From top to bottom BL, ML, HL and TPW parameters. Left) calculated directly from background ECMWF from hybrid profiles from (t+24) forecast, centre) calculated after FG step profile using as input BT_RTTOV (t+00), right) calculated after physical retrieval step profile. In all case the ground truth are the BL, ML, HL and TPW calculated from ECMWF analysis (t+00) profiles. .	20
Figure 5: BT_RTTOV FCI MTII case: LPW and TPW 2D histograms over land validation points. From top to bottom BL, ML, HL and TPW parameters. Left) calculated directly from background ECMWF from hybrid profiles from (t+24) forecast, centre) calculated after FG step profile using as input BT_RTTOV (t+00), right) calculated after physical retrieval step profile. In all case the ground truth are the BL, ML, HL and TPW calculated from ECMWF analysis (t+00) profiles. .	21
Figure 6: BT_RTTOV MSG3 case: LPW and TPW 2D histograms over sea validation points. From top to bottom BL, ML, HL and TPW parameters. Left) Calculated directly from background ECMWF from hybrid profiles from (t+24) forecast, centre) Calculated after FG step profile using as input BT_RTTOV (t+00), right) Calculated after physical retrieval step profile. In all case the ground truth are the BL, ML, HL and TPW calculated from ECMWF analysis (t+00) profiles.	22
Figure 7: BT_RTTOV MSG3 case: LPW and TPW 2D histograms over land validation points. From top to bottom BL, ML, HL and TPW parameters. Left) calculated directly from background ECMWF from hybrid profiles from (t+24) forecast, centre) Calculated after FG step profile using as input BT_RTTOV (t+00), right) Calculated after physical retrieval step profile. In all case the ground truth are the BL, ML, HL and TPW calculated from ECMWF analysis (t+00) profiles.	23
Figure 8: Real_BT FCI MTII case: LPW and TPW 2D histograms over sea validation points. From top to bottom BL, ML, HL and TPW parameters. Left) Calculated directly from background ECMWF from hybrid profiles from (t+24) forecast, centre) Calculated after FG step profile using as input using real bias corrected SEVIRI BT, right) Calculated after physical retrieval step profile. In all case the ground truth are the BL, ML, HL and TPW calculated from Hybrid ECMWF analysis(t+00) profiles.....	24
Figure 9: Real_BT FCI MTII case: LPW and TPW 2D histograms over land validation points. From top to bottom BL, ML, HL and TPW parameters. Left) Calculated directly from background ECMWF from hybrid profiles from (t+24) forecast, centre) Calculated after FG step profile using as input using real bias corrected SEVIRI BT, right) Calculated after physical retrieval step profile. In all case the ground truth are the BL, ML, HL and TPW calculated from Hybrid ECMWF analysis (t+00) profiles.....	25
Figure 10: Real_BT MSG3 case: LPW and TPW 2D histograms over sea validation points. From top to bottom BL, ML, HL and TPW parameters. Left) Calculated directly from background ECMWF from hybrid profiles from (t+24) forecast, centre) Calculated after FG step profile using as input using real bias corrected SEVIRI BT, right) Calculated after physical retrieval step profile. In all	

case the ground truth are the BL, ML, HL and TPW calculated from Hybrid ECMWF analysis($t+00$) profiles. 26

Figure 11: **Real_BT MSG3** case: LPW and TPW 2D histograms over **land** validation points. From top to bottom BL, ML, HL and TPW parameters. Left) Calculated directly from background ECMWF from hybrid profiles from ($t+24$) forecast, centre) Calculated after FG step profile using as input using real bias corrected SEVIRI BT, right) Calculated after physical retrieval step profile. In all case the ground truth are the BL, ML, HL and TPW calculated from Hybrid ECMWF analysis ($t+00$) profiles. 27

Figure 12: **BT_RTTOV FCI MTII** case: instability indices 2D histograms over **sea** validation points. From top to bottom parameters KI, LI and SHW parameters. Left) calculated directly from background ECMWF from hybrid profiles from ($t+24$) forecast, centre) calculated after FG step profile using as input using real bias corrected SEVIRI BT, right) calculated after physical retrieval step profile. In all case the ground truth are the BL, ML, HL and TPW calculated from Hybrid ECMWF analysis ($t+00$) profiles..... 28

Figure 13: **BT_RTTOV FCI MTII** case: instability indices 2D histograms over **land** validation points. From top to bottom parameters KI, LI and SHW parameters. Left) calculated directly from background ECMWF from hybrid profiles from ($t+24$) forecast, centre) calculated after FG step profile using as input using real bias corrected SEVIRI BT, right) calculated after physical retrieval step profile. In all case the ground truth are the BL, ML, HL and TPW calculated from Hybrid ECMWF analysis ($t+00$) profiles..... 29

Figure 14: **BT_RTTOV MSG3** case: instability indices 2D histograms over **sea** validation points. From top to bottom parameters KI, LI and SHW parameters. Left) calculated directly from background ECMWF from hybrid profiles from ($t+24$) forecast, centre) calculated after FG step profile using as input using real bias corrected SEVIRI BT, right) calculated after physical retrieval step profile. In all case the ground truth are the BL, ML, HL and TPW calculated from Hybrid ECMWF analysis ($t+00$) profiles..... 30

Figure 15: **BT_RTTOV MSG3** case: instability indices 2D histograms over **land** validation points. From top to bottom parameters KI, LI and SHW parameters. Left) calculated directly from background ECMWF from hybrid profiles from ($t+24$) forecast, centre) calculated after FG step profile using as input using real bias corrected SEVIRI BT, right) calculated after physical retrieval step profile. In all case the ground truth are the BL, ML, HL and TPW calculated from Hybrid ECMWF analysis ($t+00$) profiles..... 31

Figure 16: **Real_BT FCI MTII** case: instability indices 2D histograms over **sea** validation points. From top to bottom parameters KI, LI and SHW parameters. Left) calculated directly from background ECMWF from hybrid profiles from ($t+24$) forecast, centre) calculated after FG step profile using as input using real bias corrected SEVIRI BT, right) calculated after physical retrieval step profile. In all case the ground truth are the BL, ML, HL and TPW calculated from Hybrid ECMWF analysis ($t+00$) profiles..... 32

Figure 17: **Real_BT FCI MTII** case: instability indices 2D histograms over **land** validation points. From top to bottom parameters KI, LI and SHW parameters. Left) calculated directly from background ECMWF from hybrid profiles from ($t+24$) forecast, centre) calculated after FG step profile using as input using real bias corrected SEVIRI BT, right) calculated after physical retrieval step profile. In all case the ground truth are the BL, ML, HL and TPW calculated from Hybrid ECMWF analysis ($t+00$) profiles..... 33

Figure 18: **Real_BT MSG3** case: instability indices 2D histograms over **sea** validation points. From top to bottom parameters KI, LI and SHW parameters. Left) calculated directly from background ECMWF from hybrid profiles from ($t+24$) forecast, centre) calculated after FG step profile using as input using real bias corrected SEVIRI BT, right) calculated after physical retrieval step profile. In all case the ground truth are the BL, ML, HL and TPW calculated from Hybrid ECMWF analysis ($t+00$) profiles..... 34

Figure 19: **Real_BT MSG3** case: instability indices 2D histograms over **land** validation points. From top to bottom parameters KI, LI and SHW parameters. Left) calculated directly from background

ECMWF from hybrid profiles from (t+24) forecast, centre) calculated after FG step profile using as input using real bias corrected SEVIRI BT, right) calculated after physical retrieval step profile. In all case the ground truth are the BL, ML, HL and TPW calculated from Hybrid ECMWF analysis (t+00) profiles..... 35

Figure 20: **BT_RTT OV FCI MTII case:** Spatial distribution of the BL, ML, HL and TPW RMSE over validation points. From top to bottom BL, ML, HL and TPW parameters. Left) BL, ML, HL and TPW RMSE calculated directly from background ECMWF hybrid GRIB (t+24), centre) BL, ML, HL and TPW RMSE calculated after FG step profile, right) BL, ML, HL and TPW RMSE calculated after physical retrieval step profile. In all case the ground truth are the BL, ML, HL and TPW calculated from NWP-Hyb ECMWF analysis (t+00) profiles. 36

Figure 21: **BT_RTT OV MSG3 case:** Spatial distribution of the BL, ML, HL and TPW RMSE over validation points. From top to bottom BL, ML, HL and TPW parameters. Left) BL, ML, HL and TPW RMSE calculated directly from background ECMWF hybrid GRIB (t+24), centre) BL, ML, HL and TPW RMSE calculated after FG step profile, right) BL, ML, HL and TPW RMSE calculated after physical retrieval step profile. In all case the ground truth are the BL, ML, HL and TPW calculated from NWP-Hyb ECMWF analysis (t+00) profiles. 37

Figure 22: **BT_RTT OV FCI MTII case:** Same that Figure 20 but relative RMSE instead of RMSE. 38

Figure 23: **BT_RTT OV MSG3 case:** Same that Figure 21 but relative RMSE instead of RMSE..... 39

Figure 24: **Real_BT FCI MTII case:** Spatial distribution of the BL, ML, HL and TPW RMSE over validation points. From top to bottom BL, ML, HL and TPW parameters. Left) BL, ML, HL and TPW RMSE calculated directly from background ECMWF hybrid GRIB (t+24), centre) BL, ML, HL and TPW RMSE calculated after FG step profile, right) BL, ML, HL and TPW RMSE calculated after physical retrieval step profile. In all case the ground truth are the BL, ML, HL and TPW calculated from NWPHyb ECMWF analysis(t+00) profiles..... 40

Figure 25: **Real_BT MSG3 case:** Spatial distribution of the BL, ML, HL and TPW RMSE over validation points. From top to bottom BL, ML, HL and TPW parameters. Left) BL, ML, HL and TPW RMSE calculated directly from background ECMWF hybrid GRIB (t+24), centre) BL, ML, HL and TPW RMSE calculated after FG step profile, right) BL, ML, HL and TPW RMSE calculated after physical retrieval step profile. In all case the ground truth are the BL, ML, HL and TPW calculated from NWPHyb ECMWF analysis(t+00) profiles..... 41

Figure 26: **Real_BT FCI MTII case:** Same that Figure 24 but relative RMSE instead of RMSE..... 42

Figure 27: **Real_BT MSG3 case:** Same that Figure 25 but relative RMSE instead of RMSE. 43

Figure 28: **Real_BT FCI MTII case:** Spatial distribution of the KI, LI and SHW RMSE over validation points. From top to bottom KI, LI and SHW parameters. Left) RMSE calculated directly from background ECMWF hybrid GRIB (t+24), centre) RMSE calculated after FG step profile, right) RMSE calculated after physical retrieval step profile. In all case the ground truth are the KI, LI and SHW calculated from NWPHyb ECMWF analysis(t+00) profiles..... 44

Figure 29: **Real_BT MSG3 case:** Spatial distribution of the KI, LI and SHW RMSE over validation points. From top to bottom KI, LI and SHW parameters. Left) RMSE calculated directly from background ECMWF hybrid GRIB (t+24), centre) RMSE calculated after FG step profile, right) RMSE calculated after physical retrieval step profile. In all case the ground truth are the KI, LI and SHW calculated from NWPHyb ECMWF analysis(t+00) profiles. 45

Figure 30: **BT_RTT OV FCI MTII case:** RMSE profiles at different steps compared with ECMWF analysis (t+00) hybrid profiles. Top left) q RMSE on sea pixels, Top right) q RMSE on land pixels. Bottom left) T RMSE on sea pixels, Bottom right) T RMSE on land pixels. 48

Figure 31: **BT_RTT OV MSG3 case:** RMSE profiles at different steps compared with ECMWF analysis (t+00) hybrid profiles. Top left) q RMSE on sea pixels, Top right) q RMSE on land pixels. Bottom left) T RMSE on sea pixels, Bottom right) T RMSE on land pixels. 49

- Figure 32: **Real_BT_FCI_MTH** case: RMSE profiles at different steps compared with ECMWF analysis ($t+00$) hybrid profiles. Top left) q RMSE on sea pixels, Top right) q RMSE on land pixels. Bottom left) T RMSE on sea pixels, Bottom right) T RMSE on land pixels. 50
- Figure 33: **Real_BT_MSG3** case: RMSE profiles at different steps compared with ECMWF analysis ($t+00$) hybrid profiles. Top left) q RMSE on sea pixels, Top right) q RMSE on land pixels. Bottom left) T RMSE on sea pixels, Bottom right) T RMSE on land pixels. 51
- Figure 34: **BT_RTTOV_FCI_MTH** case: SKT 2D histograms. (top) sea SKT. (bottom) land SKT. Left) SKT directly from background ECMWF hybrid GRIB ($t+24$), centre) SKT calculated after FG step profile, right) SKT calculated after physical retrieval step profile. In all case the ground truth is SKT from NWP-Hyb ECMWF analysis($t+00$) profiles..... 52
- Figure 35: **BT_RTTOV_MSG3** case: SKT 2D histograms. (top) sea SKT. (bottom) land SKT. Left) SKT directly from background ECMWF hybrid GRIB ($t+24$), centre) SKT calculated after FG step profile, right) SKT calculated after physical retrieval step profile. In all case the ground truth is SKT from NWP-Hyb ECMWF analysis($t+00$) profiles..... 53
- Figure 36: **Real_BT_FCI_MTH** case: SKT 2D histograms. (top) sea SKT. (bottom) land SKT. Left) SKT directly from background ECMWF hybrid GRIB ($t+24$), centre) SKT calculated after FG step profile, right) SKT calculated after physical retrieval step profile. In all case the ground truth is SKT from NWP-Hyb ECMWF analysis($t+00$) profiles..... 53
- Figure 37: **Real_BT_MSG3** case: SKT 2D histograms. (top) sea SKT. (bottom) land SKT. Left) SKT directly from background ECMWF hybrid GRIB ($t+24$), centre) SKT calculated after FG step profile, right) SKT calculated after physical retrieval step profile. In all case the ground truth is SKT from NWP-Hyb ECMWF analysis ($t+00$) profiles. 54
- Figure 38: **BT_RTTOV_FCI_MTH** case: Spatial distribution of the SKT RMSE. (Left) SKT directly from background ECMWF hybrid GRIB ($t+24$), (centre) SKT calculated after FG non-linear regression step, (right) SKT calculated after physical retrieval step. In all case the ground truth are SKT from NWP-Hyb ECMWF analysis ($t+00$) profiles..... 54
- Figure 39: **BT_RTTOV_MSG3** case: Spatial distribution of the SKT RMSE. (Left) SKT directly from background ECMWF hybrid GRIB ($t+24$), (centre) SKT calculated after FG non-linear regression step, (right) SKT calculated after physical retrieval step. In all case the ground truth are SKT from NWP-Hyb ECMWF analysis ($t+00$) profiles..... 54
- Figure 40: **Real_BT_FCI_MTH** case: Spatial distribution of the SKT RMSE. (Left) SKT directly from background ECMWF hybrid GRIB ($t+24$), (centre) SKT calculated after FG non-linear regression step, (right) SKT calculated after physical retrieval step. In all case the ground truth are SKT from NWP-Hyb ECMWF analysis ($t+00$) profiles..... 55
- Figure 41: **Real_BT_MSG3** case: Spatial distribution of the SKT RMSE. (Left) SKT directly from background ECMWF hybrid GRIB ($t+24$), (centre) SKT calculated after FG non-linear regression step, (right) SKT calculated after physical retrieval step. In all case the ground truth are SKT from NWP-Hyb ECMWF analysis ($t+00$) profiles..... 55

1. INTRODUCTION

The EUMETSAT “Satellite Application Facilities” (SAF) are dedicated centres of excellence for processing satellite data, and form an integral part of the distributed EUMETSAT Application Ground Segment (<http://www.eumetsat.int>).

This documentation is provided by the SAF on Support to Nowcasting and Very Short Range Forecasting, hereafter NWC SAF. The main objective of NWC SAF is to provide, further develop and maintain software packages to be used for Nowcasting applications of operational meteorological satellite data by National Meteorological Services. More information can be found at the NWC SAF webpage, <http://nwc-saf.eumetsat.int>. This document is applicable to the NWC SAF processing package for geostationary meteorological satellites, NWC/GEO.

1.1 SCOPE OF THE DOCUMENT

The purpose of this document is to present the Scientific Validation results for the Clear Air Product Processor of the NWC/GEO package version 2025. The name of Clear Air Product Processor is GEO-iSHAI (imager Satellite Humidity And Instability).

The scientific validation for GEO-iSHAI version 2025 outputs has been mainly based on the validation of the GEO iSHAI parameters using as input synthetic RTTOV brightness temperatures and real bias corrected brightness temperatures for MTG-I1/FCI and SEVIRI. In the Section 2 and 3, the validation figures have been calculated from the GEO iSHAI validation datasets using temporally and spatially collocated real MTG-I1/FCI and SEVIRI and synthetic RTTOV brightness temperatures (calculated using profiles from ECMWF GRIB files on hybrid levels).

The case with synthetic BTs inputs is used to draw the main characteristics of the retrievals. The case using as input real bias BT corrected MTG-I1/FCI and SEVIRI BTs is used to show the deviation from the theoretical ones in operational conditions and to advice users on the limitations of the algorithm. To be able to make global validation and given that ECMWF analyses are of high quality, in this report these fields are taken as ground truth parameters.

In CDOP-4 or CDOP-5 more specific AHI and ABI Scientific and Validation Reports will be written.

Within this document, from now on GEO-iSHAI will only be referring to version 2025.

1.2 SOFTWARE VERSION IDENTIFICATION

The validation results presented in this document apply to the GEO iSHAI 5.0. This GEO-iSHAI version is included in the version 2025 of NWC/GEO software package.

1.3 GLOSSARY

Please refer to the “Nowcasting SAF Glossary” document in the NWC SAF web for a wider glossary and a complete list of acronyms for the NWC SAF project.

ABI	Advanced Baseline Imager
AEMET	Agencia Estatal de Meteorología Meteorology State Agency (Spain)
AHI	Advanced Himawari Imager
ASCII	American Standard Code for Information and Interchange
ATBD	Algorithm Theoretical Basis Document
BL	Precipitable water in low layer ($P_{\text{sf}} - 850 \text{ hPa}$)
BT	Brightness Temperature

CDOP (CDOP-1)	Continuous Development and Operations Phase (1)
CDOP-2	Continuous Development and Operations Phase 2
CDOP-3	Continuous Development and Operations Phase 3
CF	NetCDF Climate and Forecast (CF) Metadata Conventions
CIMSS	Cooperative Institute for Meteorological Satellite Studies (USA)
CMa	Cloud Mask
COTS	Commercial-Off-The-Shelf
CPU	Central Processor Unit
DEM	Digital Elevation Model
ECMWF	European Centre for Medium-range Weather Forecasts
EOF	Empirical Orthogonal Function
EUMETSAT	European Organisation for the Exploitation of Meteorological Satellites
FCI	Flexible Combined Imager (MTG)
FG	First Guess
FOV	Field Of View
FOR	Field Of Regard
GEO	Geostationary Satellites
GEO-CMa	GEO Cloud Mask and Cloud Amount
GEO-iSHAI	GEO imaging Satellite Humidity And Instability
GRIB	Gridded Information in Binary Form
HDF5	Hierarchical Data format version 5
HL	Precipitable water in High Layer (500 – 0 hPa)
hPa	Hecto Pascal
HRIT	High Rate Image Transmission
IDL	Interactive Data Language
IR	InfraRed
IREMIS	InfraRed Emissivity
IRS	Infrared Sounder (MTG)
iSHAI	imaging Satellite Humidity And Instability
K	Kelvin
KI	K-Index
km	kilometre
LI	Lifted Index
LPW	Layer Precipitable Water
LST	Land Surface Temperature
MARS	ECMWF Meteorological Archive and Retrieval Facility
McIDAS	Man Computer Interactive Data Access System
ML	Precipitable water in Medium Layer (850 – 500 hPa)
MSG	Meteosat Second Generation

MTG	Meteosat Third Generation
MTG-FCI	Meteosat Third Generation Flexible Combined Imager
MTG-IRS	Meteosat Third Generation Infra Red Sounder
netCDF	Network Common Data Form
NRT	Near Real Time
NWC	Nowcasting
NWC/GEO	Geostationary part of the Nowcasting SAF
NWCLIB	Nowcasting Library
NWC SAF	Nowcasting SAF
NWP	Numerical Weather Prediction
NWP SAF	SAF for Numerical Weather Prediction
LPW	Layer Precipitable Water
PGE	Product Generation Element
	PGE01 Cloud Mask (GEO-CMa) Product Generator
	PGE13 SEVIRI Physical Retrieval (SPhR) Product Generator
PW	Precipitable Water
RTM	Radiative Transfer Model
RTTOV	Radiative Transfer for TOVs
SAF	Satellite Application Facility
SEVIRI	Spinning Enhanced Visible InfraRed Imager
SG	Steering Group
SHAI	Satellite Humidity And Instability
SHW	Showalter Index
SKT	Skin Temperature
SST	Sea Surface Temperature
SW	Software
TOZ	Total ozone
TPW	Total Precipitable Water
TM	Task Manager
UM	User Manual
VR	Validation Report
VSA	Visiting Scientist Activities
WV	Water Vapour Channel

1.4 REFERENCES

1.4.1 NWC SAF Applicable Documents

The following documents, of the exact issue shown, form part of this document to the extent specified herein. Applicable documents are those referenced in the Contract or approved by the Approval Authority. They are referenced in this document in the form [AD.X]

For versioned references, subsequent amendments to, or revisions of, any of these publications do not apply. For unversioned references, the current edition of the document referred applies.

Current documentation can be found at the NWC SAF Helpdesk web: <http://nwc-saf.eumetsat.int>.

Ref.	Title	Code	Version
[AD.1]	Proposal for the Fourth Continuous Development and Operations Phase (CDOP4)	NWC/SAF/AEMET/MGT/CDO4Proposal	1.0
[AD.2]	NWCSAF Project Plan	NWC/CDOP4/SAF/AEMET/MGT/PP	3.0.0
[AD.3]	Configuration Management Plan for the NWCSAF	NWC/CDOP4/SAF/AEMET/MGT/CMP	1.2.0
[AD.4]	NWCSAF Product Requirements Document	NWC/CDOP4/SAF/AEMET/MGT/PRD	3.0.0

Table 1: List of Applicable Documents.

The reference documents contain useful information related to the subject of the project. These reference documents complement the applicable ones, and can be looked up to enhance the information included in this document if it is desired. They are referenced in this document in the form [RD.X]

For dated references, subsequent amendments to, or revisions of, any of these publications do not apply. For undated references, the current edition of the document referred applies.

1.4.2 Reference Documents

Ref.	Title	Code	Vers
[RD.1]	Algorithm Theoretical Basis Document for iSHAI Product Processors of the NWC/GEO MTG-I Day-1	NWC/CDOP2/MTG/AEMET/SCI/ATBD/iSHAI	1.1.0
[RD.2]	User Manual for iSHAI Product Processors of the NWC/GEO MTG-I Day-1	NWC/CDOP3/MTG/AEMET/SCI/UM/iSHAI	1.2.0
[RD.3]	Data Output Format for the NWC/GEO MTG-I day-1	NWC/CDOP2/MTG/AEMET/SW/DOF	1.4.0
[RD.4]	System and Components Requirements Document for the NWC/GEO MTG-I day-1	NWC/CDOP2/MTG/AEMET/SW/SCRD	1.3.1
[RD.5]	Interface Control Document for Internal and External Interfaces of the NWC/GEO MTG-I day-1	NWC/CDOP2/MTG/AEMET/SW/ICD/1	1.4.0
[RD.6]	Interface Control Document for the NWCLIB of the NWC/GEO MTG-I day-1	NWC/CDOP2/MTG/AEMET/SW/ICD/2	1.4.0
[RD.7]	User Manual for the NWC/GEO: Software Part	NWC/CDOP3/MTG/AEMET/SW/UM	1.3.0

Table 2: List of Referenced Documents

2. MTG-I1/FCI AND SEVIRI GEO-ISHAI VALIDATION DATASET

2.1 DESCRIPTION OF FILES USED

Validation is continuous and important task for us. As example, the first construction of one training and validation dataset was started in 31 December 2007. Since the resolution and files has evolved with time, in this document the ones used in this Validation Report are described.

In order to build the GEO-iSHAI datasets for training and validation purposes, real data from MTG-I1/FCI and MSG SEVIRI images and ECMWF GRIB files have been used. The period used in the Validation Report is from 25th July 2024 to 31st January 2025. Together with daily store of FCI and SEVIRI images it is made the daily request of ECMWF on ECMWF MARS as described below.

At the time of writing this report the input data files available for training, tuning and validation activities are:

From ECMWF fields:

- 00 Z and 12 Z runs
- analysis ($t+00$ hours) and ($t+12$ hours) and ($t+24$ hours) forecasts
- region: global for absolute latitude less than 65°. That is NW corner at (65° N, 180° W) and SE corner at (65° S, 179.8° E). The broad region allows to generate training and validation dataset with other GEO satellites than the operational MSG at 0° with slight modifications of the code.
- time period: from 25th July 2024 00 Z to present of each day during this period. The database is updated every day.
- horizontal resolution: 0.2° by 0.2°
- vertical resolution: two different vertical resolutions are used
 - o Hybrid levels (hereafter denoted as NWP-Hyb): The number is 137 levels.
 - o Fixed pressure levels (hereafter denoted as NWP-P): These GRIB files are needed only for Cloud Mask (CMA) processing. The pressure levels available on MARS are typically 15 or 25 synoptic levels (as example: 1000, 925, 850, 700, 500, 400, 300, 250, 200, 150, 100 .. hPa)

Note: the NWP-P GRIB files are the ones used as input to the NWCSAF software package and needed here just for CMA generation.

- parameters: temperature (T) profile, humidity profile (specific humidity [q] for NWP-Hyb and relative humidity [RH] for NWP-P files), ozone profile, skin temperature.

Note: when the collocated records are written, the NWP($t+24$) from previous 24 hours ECMWF run, the NWP($t+12$) from previous 12 hours ECMWF run are collocated in the same record with the NWP($t+00$). As example, the 01 January at 00UTC NPW($t+00$) analysis profile is collocated in the same record than the one with the NWP($t+24$) from 31 December 00 UTC run and the NWP($t+12$) from 31 December 12 UTC run.

From MTG-I1/FCI and MSG/SEVIRI Observations:

- 00 Z and 12 Z slots
- region: MTG-I1/FCI region of 4500 x 4500 IR pixels centred at subsatellite position and SEVIRI MSG/SEVIRI region of 3400 x 3400 IR pixels centred at subsatellite position (only pixels with satellite zenith angle lower than 70°)
- time period: from 25th July 2024 to present of each day during this period (continuous update) but in this Validation Report it has been used till the 31st January 2025

- horizontal resolution: MTG-I1/FCI and MSG/SEVIRI full IR resolution and their satellite projections
- MTG-I1/FCI: All FCI IR/WV channels
- SEVIRI channels: All SEVIRI IR/WV channels. Currently in the validation datasets there are used MSG data from MSG-3.
- Hereafter real data are brightness temperatures (BTs).

These are the dynamic information datasets used for the tuning and validation activities. Specific datasets used for different objectives are in part generated from them and descriptions are provided in the respective sections.

In order to make a better comparison of MTI1/FCI and MSG3/SEVIRI it was made a further screening in order to use only pixels present in both MTI1/FCI and MSG3/SEVIRI. That means that it has been generated a collocated MTI1/FCI and MSG3/SEVIRI training and validation dataset.

2.2 DESCRIPTION OF PROCESS TO GENERATE THE VALIDATION DATASET

The core of the process is the same than in the Validation Reports of previous iSHAI versions. It has been followed the same process since it is still valid and it has been maintained. To build one good validation and training dataset is a high priority and standing task for us. The process to build the GEO-iSHAI v2025 validation dataset is a heritage of the process used to build previous versions of the PGE13 SPhR and iSHAI validation dataset.

The main idea is to generate the whole validation dataset using the NWCSAF GEO Cloud Mask (CMA) program and a modified version of GEO-iSHAI software called PGE00 which also uses RTTOV-13 for an efficient generation of collocated real and synthetic BTs.

PGE00 and GEO-iSHAI allow activating an option in their configuration files to write at clear pixels in optional binary files structures with real satellite BTs together with the T, q and O₃ profiles, surface and ancillary parameters collocated spatially, temporally and vertically interpolated to the position and time of the clear satellite pixels. The optional binary files of GEO-iSHAI just save the MTG-I1/FCI or MSG/SEVIRI IR channels used in iSHAI algorithm; but PGE00 is configured to save the full set of 8 MTG-I1/FCI or MSG/SEVIRI IR channels.

The use of RTTOV-13 implies that the GEO-iSHAI validation dataset is based on profiles with 54 pressure levels. It has been used NWC/GEO v2025. Thus, all the profiles used in the validation have similar characteristics to the profiles used and retrieved within the GEO-iSHAI v2025 execution in operational mode.

The period chosen as the reference period for this early GEO-iSHAI validation dataset was the first with a stable dissemination of real FCI. It is short and it would be desirable to make later another with a long period of at least one year. The validation results obtained using as ground truth the ECMWF NWPHyb analysis ($t+00$) profiles are presented here. In section 3, the validation results using as input to GEO-iSHAI real bias BT corrected FCI or SEVIRI BTs are also included in order to show the deviation from the theoretical ones and to advice users on the limitation of the algorithm.

Positions of GEO iSHAI validation dataset: For GEO iSHAI parameters validation, a set of predefined positions of a 1° x 1° grid plus the RAOB stations positions have been chosen. The set contains 13001 points in the actual mask. The positions where validation is made can be seen in Figure 1.

Process to build the GEO iSHAI validation dataset: The actual process to build the validation and training dataset is the following:

a) Calculate Cloud Mask (GEO-CMa): the cloud mask generation is the first step. The GEO-CMA program is first executed. The results of GEO-CMA program are netCDF files with the cloud mask located at *SSAFNWC/export/CMA*.

GEO-CMA for MSG/SEVIRI has been used for MSG/SEVIRI processing and GEO-CMA for MTI1/FCI has been used for MTI1 processing. Please, note that for CMA the NWP GRIB files used as input need to be on fixed pressure levels whilst for this Validation Report all calculations come from hybrid ECMWF GRIB files (137 hybrid levels). In this report all background NWP profiles have been downloaded from ECMWF.

b) Selection of clear validation locations by screening the cloud mask: the CMA cloud mask file is overwritten with the multiplication of CMA mask with the 13001 validation position mask (1 for selected pixel and 0 in the rest). The use of this screened cloud mask speeds up later the GEO-iSHAI and PGE00 process because instead of executing the physical retrieval over several millions of clear air pixels it is executed only over the clear air pixels among the 13001 predefined positions.

The process to get the screened cloud mask is:

- the cloud mask matrix is read from the CMA file
- the cloud mask matrix is multiplied with the 13001 validation positions mask (matrix with same dimensions of CMA with values: 1 for validation points and 0 for the rest of pixels) and the result is the screened cloud mask.
- This screened cloud mask is used to overwrite the CMA cloud mask netCDF file on *SSAFNWC/export/CMA*.

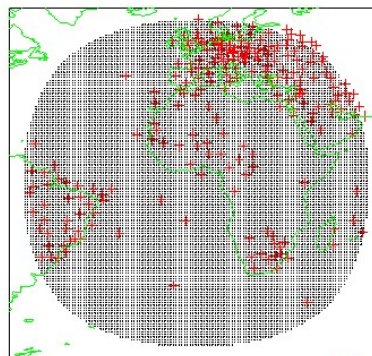


Figure 1: Predefined set of 13001 validation points used in validation datasets. Grid network of 1° x 1° plus Radiosonde Stations (red crosses).

c) To obtain the collocated profiles from analysis ($t+00$), ($t+12$) forecast and ($t+24$) forecast: the PGE00 program is executed three times for each slot. The PGE00 program calculates the profiles by interpolating the ECMWF fields from hybrid levels to 54 levels in the vertical and also in time and space. It also calls RTTOV-13 to calculate the synthetic BTs.

In the first PGE00 execution: the screened cloud mask, the real FCI or SEVIRI image and as background NWP the ECMW $t+00$ analysis GRIB file (hereafter denoted as NWPH00) are used as inputs.

In the second PGE00 execution: the screened cloud mask, the FCI or SEVIRI image and as background NWP-Hyb the $t+12$ forecast ECMWF GRIB file from previous 12 hour ECMWF run (hereafter denoted as NWPH12) are used as inputs.

In the third PGE00 execution: the screened cloud mask, the FCI or SEVIRI image and as background NWP the ECMW $t+24$ forecast ECMWF GRIB file (hereafter denoted as NWPH24) are used as inputs.

In the first execution it is read the (T, q, O₃) profiles and some surface parameters at the clear air predefined positions from ECMWF $t+00$ analysis.

With the second execution it is read the (T , q , O_3) profiles and some surface parameters (P_{sfc} , T_{skin} , etc), from the $\$SAFNWC/tmp$ binary files, at the clear air predefined positions from $t+12$ hours ECMWF forecast.

With the third execution it is read the (T , q , O_3) profiles and some surface parameters (P_{sfc} , T_{skin} , etc), from the $\$SAFNWC/tmp$ binary files, at the clear air predefined positions from $t+24$ hours ECMWF forecast.

Together with the $t+00$, $t+12$ and $t+24$ profiles, ancillary data (as emissivities, longitude, latitude, zenith angle, etc) are also read from the $\$SAFNWC/tmp$ binary files. The process (for ($t+00$) and ($t+12$) cases) can be seen in Figure 2. The result is one binary file by slot that can be easily read on IDL with the *restore* command. The mean number of retained clear pixels by slot is around 4700 pixels.

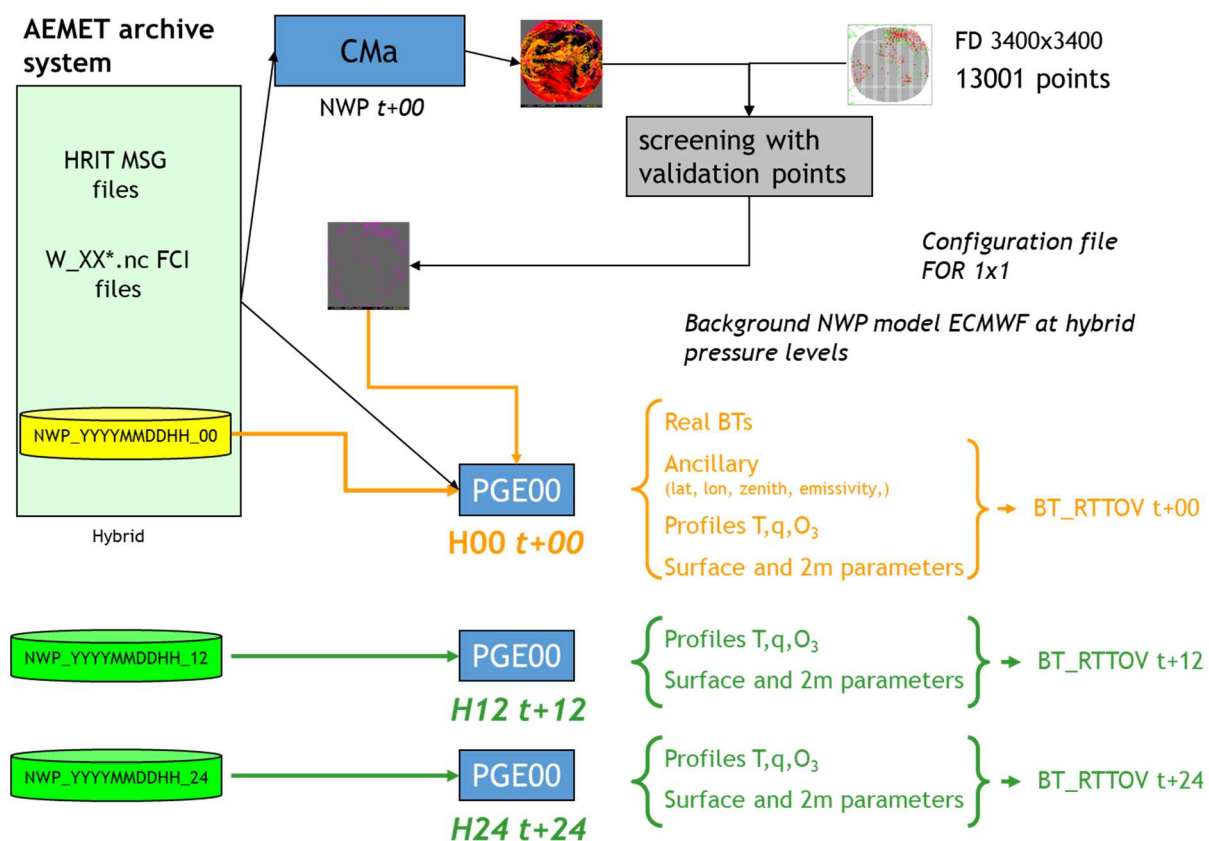


Figure 2: Generation of the records for adding to GEO iSHAI validation dataset from one image for ($t+00$), ($t+12$) and ($t+24$) cases for MTI1/FCI and MSG3/SEVIRI.

d) Joining the files for every slot on monthly files: In order to allow an easy management of the datasets, the slot binary files are joined in one file for every month. It is made with one IDL procedure. This monthly binary files are the base for the validation process since files on a monthly basis can be joined easily to build a wider period dataset. The number of pixels used here is 300000 pixels per month (if completed).

e) Joining the monthly files on a period file: Once a period is selected for validation or training, one period binary file is generated joining the monthly files for the months in the period. It is made with one IDL procedure. In this validation report it has been used 1 out 3 clear pixels.

f) Write binary file which can be used as input to the validation version of GEO-iSHAI: One array with selected parameters is written on a binary file in a format that will be used later with the ad hoc version of GEO-iSHAI for validation. This validation version processes the data record by record instead of processing a region of a satellite image, as is done in the GEO-iSHAI operational version.

g) Execute the ad hoc validation version of the GEO-iSHAI software: to get an assessment of the new coefficients for the First-Guess (hereafter FG) regression and the physical retrieval steps of 2025 GEO-iSHAI, one ad hoc validation version of the sources of GEO-iSHAI to process iSHAI algorithm and RTTOV-13 on record by record basis has been developed. Thus, it is possible to test the new FG regressions coefficients, Empirical Orthogonal Function (EOF) coefficients files, E^{-1} and B^{-1} matrices, avoiding the huge task to reprocess from the complete HRIT SEVIRI files and ECMWF GRIB files.

This also allows to choose as input to the algorithm real FCI or SEVIRI BTs (bias corrected or uncorrected) or synthetic RTTOV FCI or SEVIRI BTs. The outputs of this validation program are the profiles after FG regression and/or physical retrieval steps using as inputs the GEO-iSHAI validation dataset profiles. This process allows testing new version of iSHAI software or new coefficients just over GEO-iSHAI validation dataset before implementing it in the GEO-iSHAI operational software. This process is a natural consequence from previous experiences.

h) Build the GEO iSHAI validation dataset: The outputs of the previous step are blended with the structures of the validation dataset (ancillary fields as emissivity values, land/sea mask, height, etc.) and one IDL binary file for restoring is generated.

Structure of the records in the GEO iSHAI validation dataset: After the execution of the previous steps the validation dataset for a period is one array (that could contains several millions of records in a future wider period) written on an IDL binary file. The array can be restored easily with the use of IDL command *restore*. Every record is one IDL structure with the following parameters or fields:

- **Ancillary**: longitude, latitude, emissivity values, etc.
- **Date**: day, year, hour, etc.
- **NWP from ECMWF analysis ($t+00$)**: ECMWF temperature and humidity profiles interpolated to the 54 RTTOV pressure levels interpolated vertically from 137 hybrid levels, T_{skin} , pressure at surface, etc. from the analyses ($t+00$) ECMWF GRIB files. It will be used as the validation truth.
- **NWP from ECMWF forecast ($t+12$)**: ECMWF temperature and humidity profiles interpolated to the 54 RTTOV pressure levels interpolated vertically from 137 hybrid levels, T_{skin} , pressure at surface, etc. from the previous run to the image ECMWF $t+12$ forecast (as example for image 20250101 at 00Z the $t+12$ forecast from 20241231 at 12 UTC ECMWF run is used).
- **NWP from ECMWF forecast ($t+24$)**: ECMWF temperature and humidity profiles interpolated to the 54 RTTOV pressure levels interpolated vertically from 137 hybrid levels, T_{skin} , pressure at surface, etc. from the previous run to the image ECMWF $t+24$ forecast (as example for image 20250101 at 00Z the $t+24$ forecast from 20241231 at 00 UTC ECMWF run is used).
- **BT_SEVIRI(8)**: uncorrected BT from HRIT file. $BT_SEVIRI[IR3.9, WV6.2, WV7.3, IR10.8, IR8.7, IR9.7, IR12.0, IR13.4]$.
- **SEVIRI BT_RTTOV(8) from NWPHyb($t+00$)**: Synthetic BTs calculated using the RTTOV-11.2 with the analysis ($t+00$). $H00.BT_RTTOV[IR3.9, WV6.2, WV7.3, IR10.8, IR8.7, IR9.7, IR12.0, IR13.4]$.
- **SEVIRI BT_RTTOV(8) from NWPHyb($t+12$)**: Synthetic BTs calculated using the RTTOV-11.2 with the forecast ($t+12$). $H12.BT_RTTOV[IR3.9, WV6.2, WV7.3, IR10.8, IR8.7, IR9.7, IR12.0, IR13.4]$.
- **SEVIRI BT_RTTOV(8) from NWPHyb($t+24$)**: Synthetic BTs calculated using the RTTOV-11.2 with the forecast ($t+24$). $H24.BT_RTTOV[IR3.9, WV6.2, WV7.3, IR10.8, IR8.7, IR9.7, IR12.0, IR13.4]$.
- **FCI BT_RTTOV(8) from NWPHyb($t+00$)**: Synthetic BTs calculated using the RTTOV-11.2 with the analysis ($t+00$). $H00.BT_RTTOV[IR3.8, WV6.3, WV7.3, IR8.7, IR9.6, IR10.5, IR12.3, IR13.3]$.
- **FCI BT_RTTOV(8) from NWPHyb($t+12$)**: Synthetic BTs calculated using the RTTOV-11.2 with the forecast ($t+12$). $H12.BT_RTTOV[IR3.8, WV6.3, WV7.3, IR8.7, IR9.6, IR10.5, IR12.3, IR13.3]$.
- **FCI BT_RTTOV(8) from NWPHyb($t+24$)**: Synthetic BTs calculated using the RTTOV-11.2 with the forecast ($t+24$). $H24.BT_RTTOV[IR3.8, WV6.3, WV7.3, IR8.7, IR9.6, IR10.5, IR12.3, IR13.3]$.
- **Same for other GEO imagers or MTG-IRS or IASI**

In order to make a better comparison of MTI1/FCI and MSG3/SEVIRI it was made a further screening in order to use only pixels present in both MTI1/FCI and MSG3/SEVIRI. That means that it has been estimated clear in both chains. Thus it has been generated a collocated MTI1/FCI and MSG3/SEVIRI training and validation dataset.

These basic validation and training datasets have been used for several tasks. One of them consisting of splitting the records in the global dataset into records to generate the validation datasets (1 out 3 positions with offset 0) and the training ones (1 out 3 positions with offset 1). All the 2025 versions of GEO-iSHAI coefficients have been calculated with this dataset. It has been also used for tuning of SEVIRI RGBs recipes to FCI RGBs recipes.

To avoid some issues (as FCI or SEVIRI BT biases, emissivity, contamination by clouds, need of screening in the selection of the records, etc.) and to make the document more readable, the assessment of the performances for these new GEO-iSHAI coefficients files is shown first when GEO-iSHAI uses as input synthetic RTTOV brightness temperatures from ECMWF hybrid analysis ($t+00$) profiles; this experiment is denoted hereafter as **BT_RTTOV case**. **It is made for both FCI and SEVIRI cases.**

Then, the performances are compared with the ones using as input to GEO-iSHAI real bias corrected FCI or SEVIRI BTs; this experiment is denoted hereafter as *Real_BT* on the text. **But on the images it appears as SEVIRI case; this is due to fact that it has been reused software from previous validation activities of SEVIRI and it was used SEVIRI string as indication of real BTs.** To correct this for FCI case was too much complicated due to the lack of time.

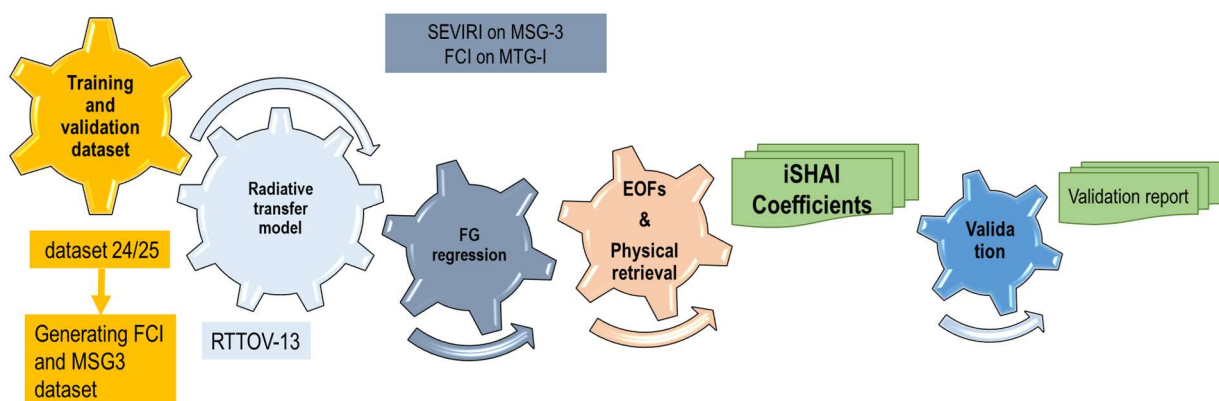


Figure 3: GEO iSHAI validation scheme.

3. VALIDATION RESULTS

In all cases the figures and statistical performance are shown from the validation of analysis $t+00$ versus $t+24$ forecast. The reason to show the performance of $t+24$ instead of the performance of $t+12$ is that with the high performance of the ECMWF model the separation of lines in rmse profiles and the difference in colour for spatial figures were too narrow on $t+12$ forecast to appreciate them. The performance of analysis $t+00$ versus $t+12$ forecast is available and could be asked to mmartinezr@aemet.es.

In all the figures and statistical performance the validation dataset used is the collocated FCI and SEVIRI from 25th July 2024 to 31st January 2025 for a full comparison of the performance of iSHAI with both instrument.

In order to assess the performance of iSHAI algorithm it has been made three main validation tests:

1. **Synthetic RTTOV BTs** calculated using as input to RTTOV the ECMWF analysis $t+00$ profiles are used as input to the GEO iSHAI and it is denoted hereafter as **BT RTTOV case**. It is used to draw the main characteristics of iSHAI and to estimate the potential performance. In this synthetic case the main advantage is that the analysis ($t+00$ forecast) can be considered as a real truth and the calculated statistical parameters can be used to assess the statistical performance of iSHAI.
2. **Real bias corrected FCI or SEVIRI BTs** are used as input to the GEO iSHAI and it is denoted hereafter as **Real BT case**. **In the images appear BT_SEVIRI due to reuse of software for SEVIRI case as indicator of the use of real satellite data (FCI or SEVIRI)**. It is used to show the deviation from the theoretical one in operational conditions; the calculated statistical parameters in this case has the disadvantage to have no real truth. Thus, the difference in the fields with RTTOV case are due to noise in satellite, errors in RTTOV and errors in iSHAI coefficients in one hand and the lack of a real truth to compare in another. As an example, the source of the differences on the SKT over land field in **Real BT case** compared with the one in **BT RTTOV case** are due to the fact that real SKT is not well represented by ECMWF analysis SKT (there is no truth) and second the errors introduced by iSHAI con SKT estimation due to the errors mentioned above.
3. **Real SEVIRI BTs without bias BT correction** are used as input to the GEO iSHAI and it is denoted hereafter as **BT SEVIRI unc case**. It is used internally to assess the stability of iSHAI algorithm and to advice users on the limitations of the algorithm. The results are not shown here.

3.1 2D DIMENSIONAL HISTOGRAMS OF GEO iSHAI PARAMETERS

It has been used always as truth the ECMWF analysis denoted here as NWP-Hyb ($t+00$) profiles. The 2D dimensional histograms of the iSHAI parameters compared with the same parameter calculated from the ECMWF analysis ($t+00$) are shown in this Section. It has been generated for both FCI and SEVIRI instruments. Thus, it can be compared the performances of iSHAI fields from FCI and SEVIRI instruments. It has been calculated independently for sea and land pixels.

First Figures are for **BT RTTOV case** in order to show that the theoretical performances of iSHAI of FCI and SEVIRI are similar. Then, same Figures but for **Real BT case** can be seen. The statistical values (RMSE, bias and correlation) appear in the 2D histograms.

Note that GEO-iSHAI BL is the precipitable water in a layer between P_{sfc} to 850 hPa. GEO-iSHAI ML is the precipitable water in a layer between 850 hPa to 500 hPa. GEO iSHAI HL is the precipitable water in a layer between 500 hPa to 0.1 hPa. GEO iSHAI TPW is the total precipitable water i.e the precipitable water in a layer between P_{sfc} to 0.1 hPa.

The parameters with the largest added value are ML and HL parameters; this fact is due to the WV channels. Other important result is that the 2D histograms of the GEO-iSHAI parameters show no significant bias and it is not needed any post processing correction.

In the case of *Real_BT* case over land some spread in the 2D histograms shows up; the cause of this spread could be due to the factors mentioned before (cloud contaminated pixels, uncertainties in the emissivity atlases, disagreements in the skin temperature from the ECMWF, etc).

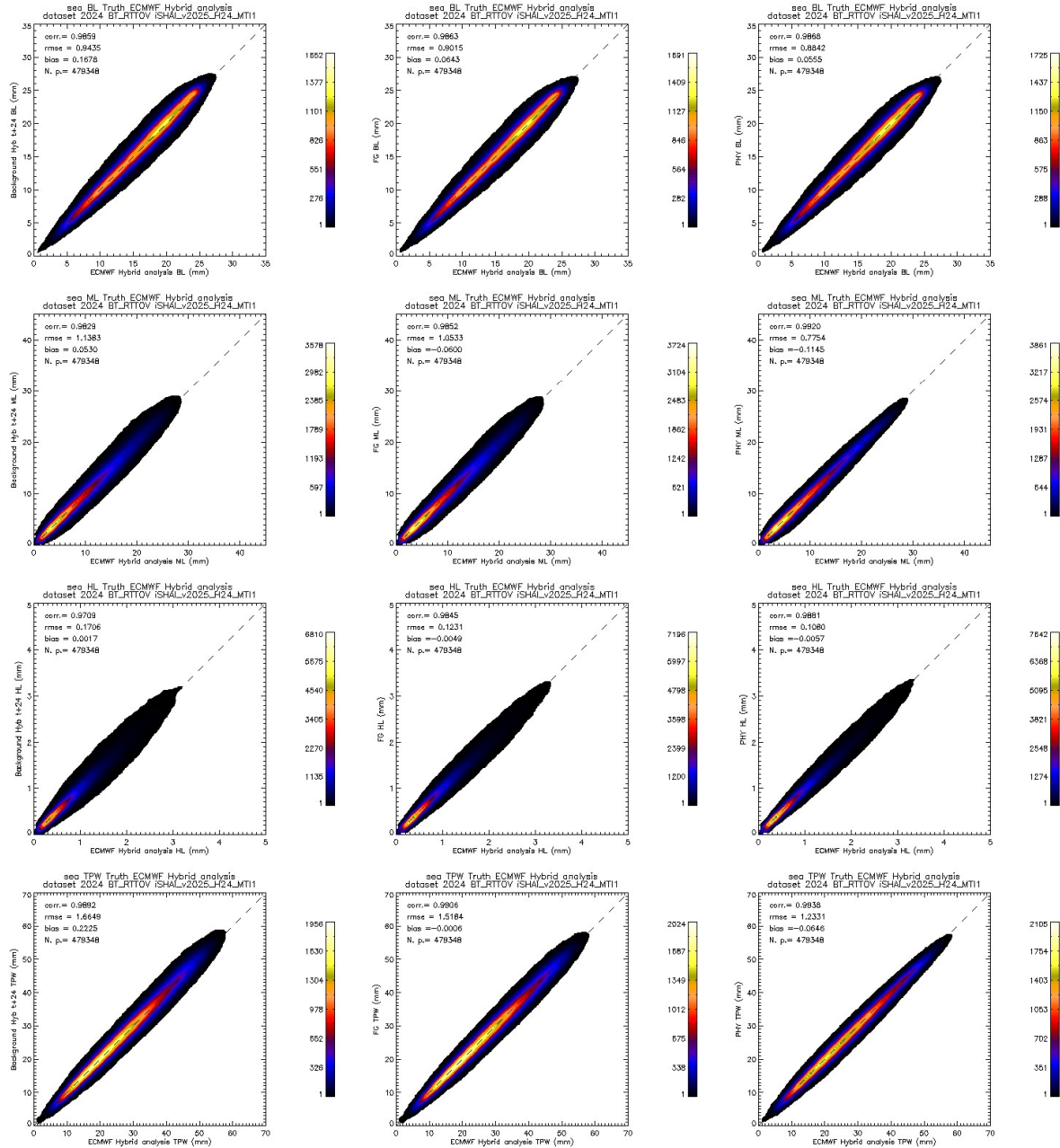


Figure 4: *BT_RTTOV FCI MTI1* case: LPW and TPW 2D histograms over *sea* validation points. From top to bottom BL, ML, HL and TPW parameters. Left) calculated directly from background ECMWF from hybrid profiles from (t+24) forecast, centre) calculated after FG step profile using as input *BT_RTTOV* (t+00), right) calculated after physical retrieval step profile. In all case the ground truth are the BL, ML, HL and TPW calculated from ECMWF analysis (t+00) profiles.

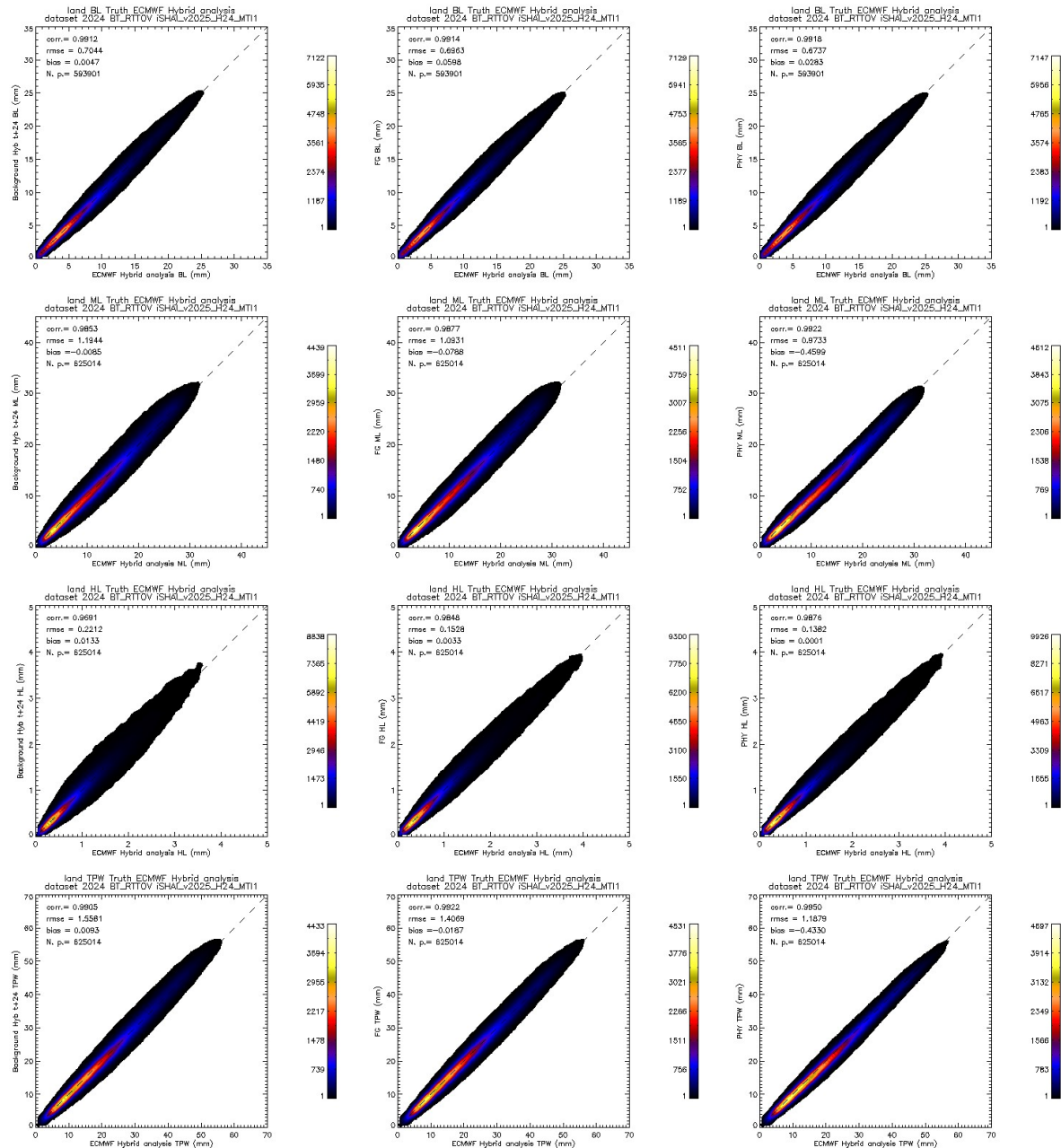


Figure 5: BT_RTTOV FCI MTI1 case: LPW and TPW 2D histograms over land validation points. From top to bottom BL, ML, HL and TPW parameters. Left) calculated directly from background ECMWF from hybrid profiles from (t+24) forecast, centre) calculated after FG step profile using as input BT_RTTOV (t+00), right) calculated after physical retrieval step profile. In all case the ground truth are the BL, ML, HL and TPW calculated from ECMWF analysis (t+00) profiles.

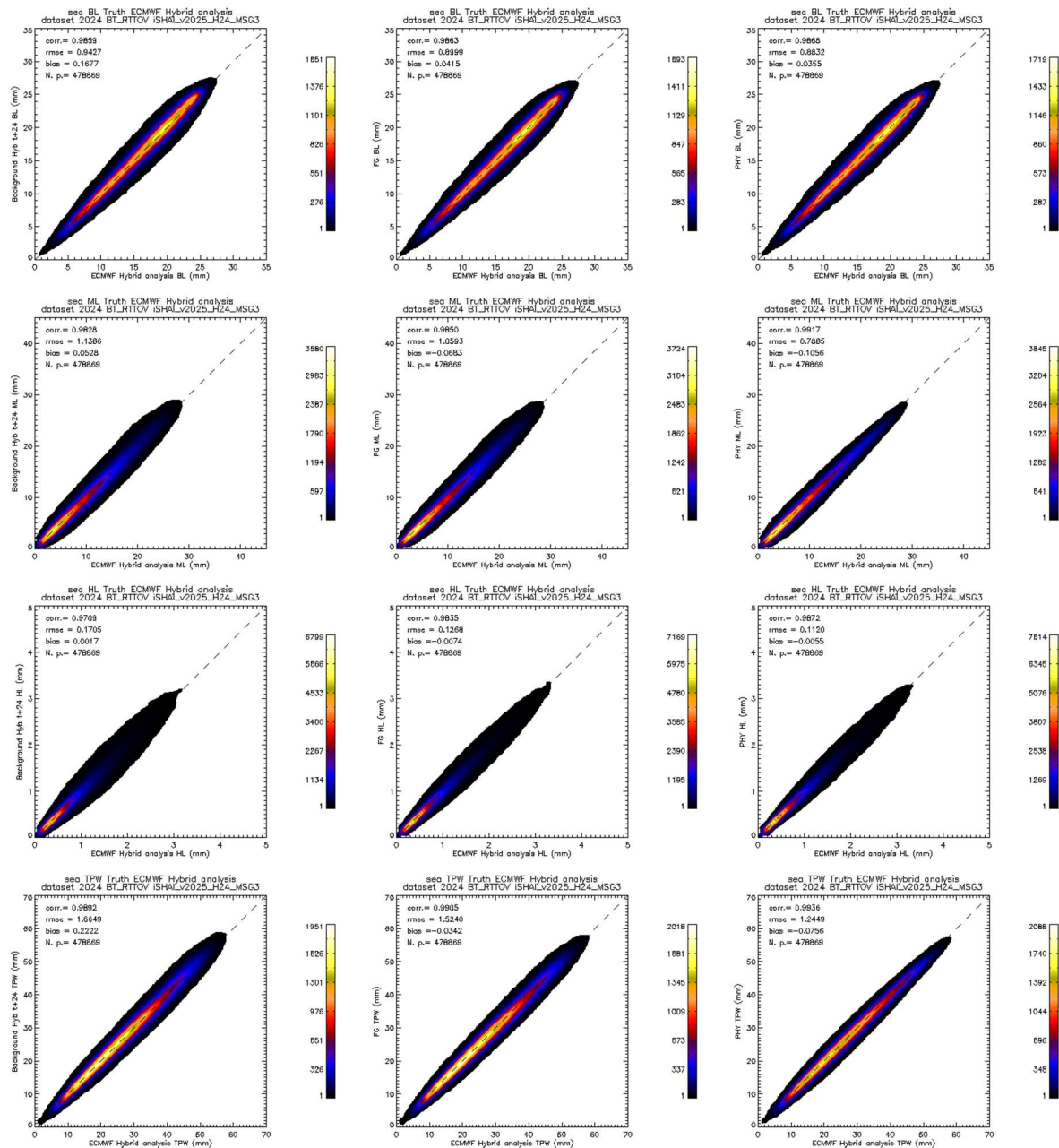


Figure 6: *BT_RTTOV MSG3* case: LPW and TPW 2D histograms over *sea* validation points. From top to bottom BL, ML, HL and TPW parameters. Left) Calculated directly from background ECMWF from hybrid profiles from (t+24) forecast, centre) Calculated after FG step profile using as input BT_RTTOV (t+00), right) Calculated after physical retrieval step profile. In all case the ground truth are the BL, ML, HL and TPW calculated from ECMWF analysis (t+00) profiles.

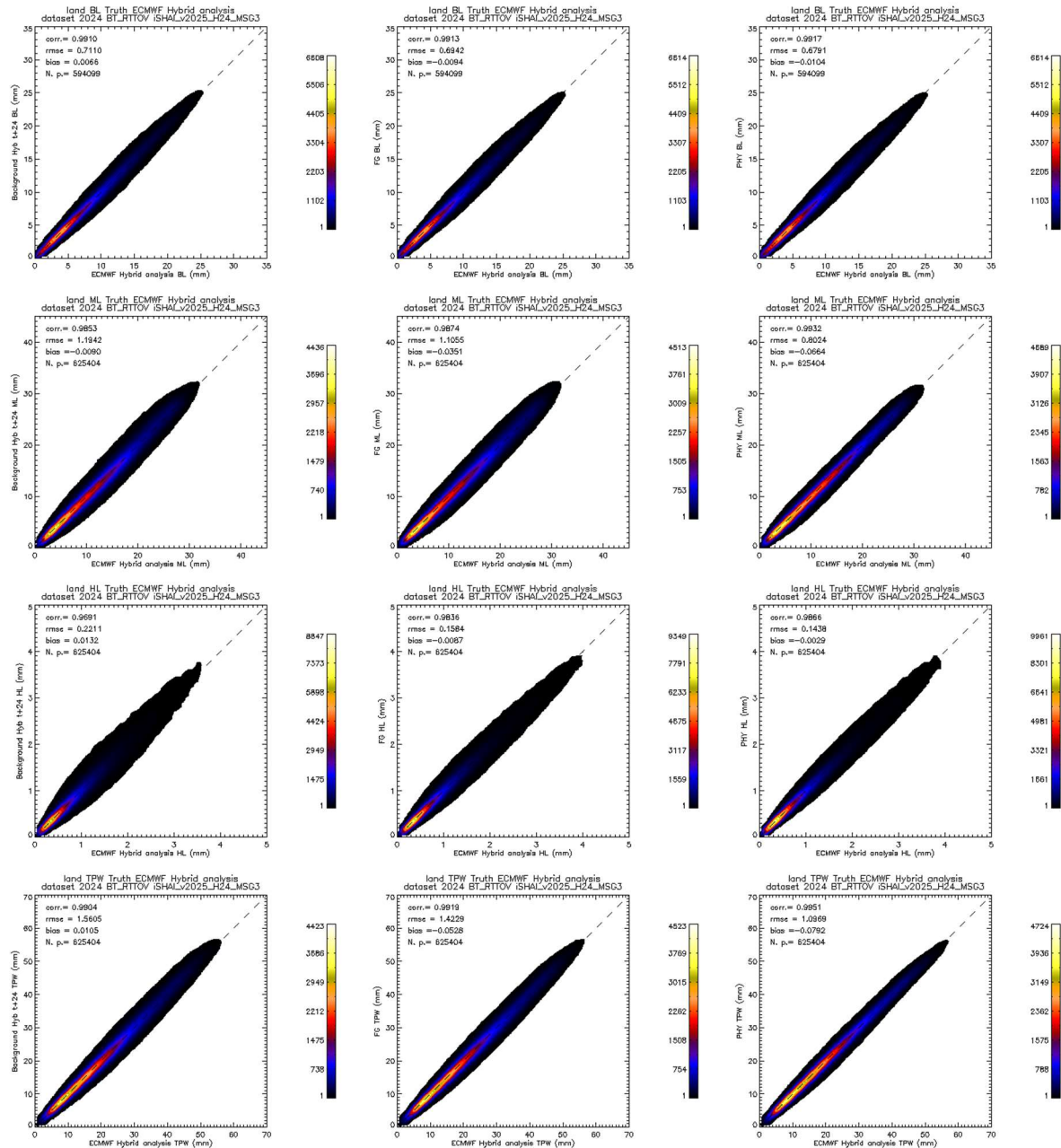


Figure 7: **BT_RTTOV MSG3** case: LPW and TPW 2D histograms over *land* validation points. From top to bottom BL, ML, HL and TPW parameters. Left) calculated directly from background ECMWF from hybrid profiles from (t+24) forecast, centre) Calculated after FG step profile using as input BT_RTTOV (t+00), right) Calculated after physical retrieval step profile. In all case the ground truth are the BL, ML, HL and TPW calculated from ECMWF analysis (t+00) profiles.

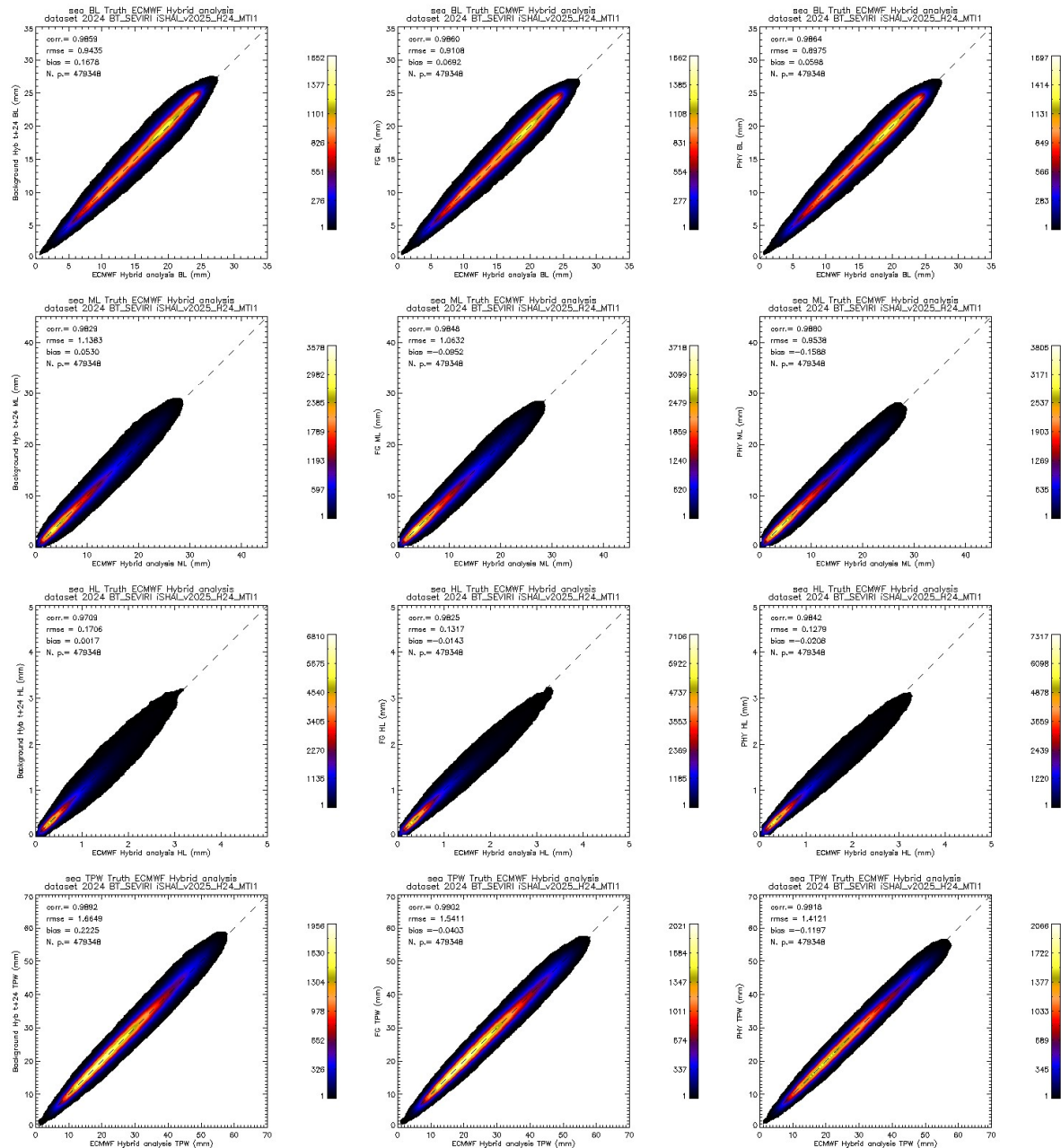


Figure 8: Real_BT FCI MTI1 case: LPW and TPW 2D histograms over sea validation points. From top to bottom BL, ML, HL and TPW parameters. Left) Calculated directly from background ECMWF from hybrid profiles from (t+24) forecast, centre) Calculated after FG step profile using as input using real bias corrected SEVIRI BT, right) Calculated after physical retrieval step profile. In all case the ground truth are the BL, ML, HL and TPW calculated from Hybrid ECMWF analysis(t+00) profiles.

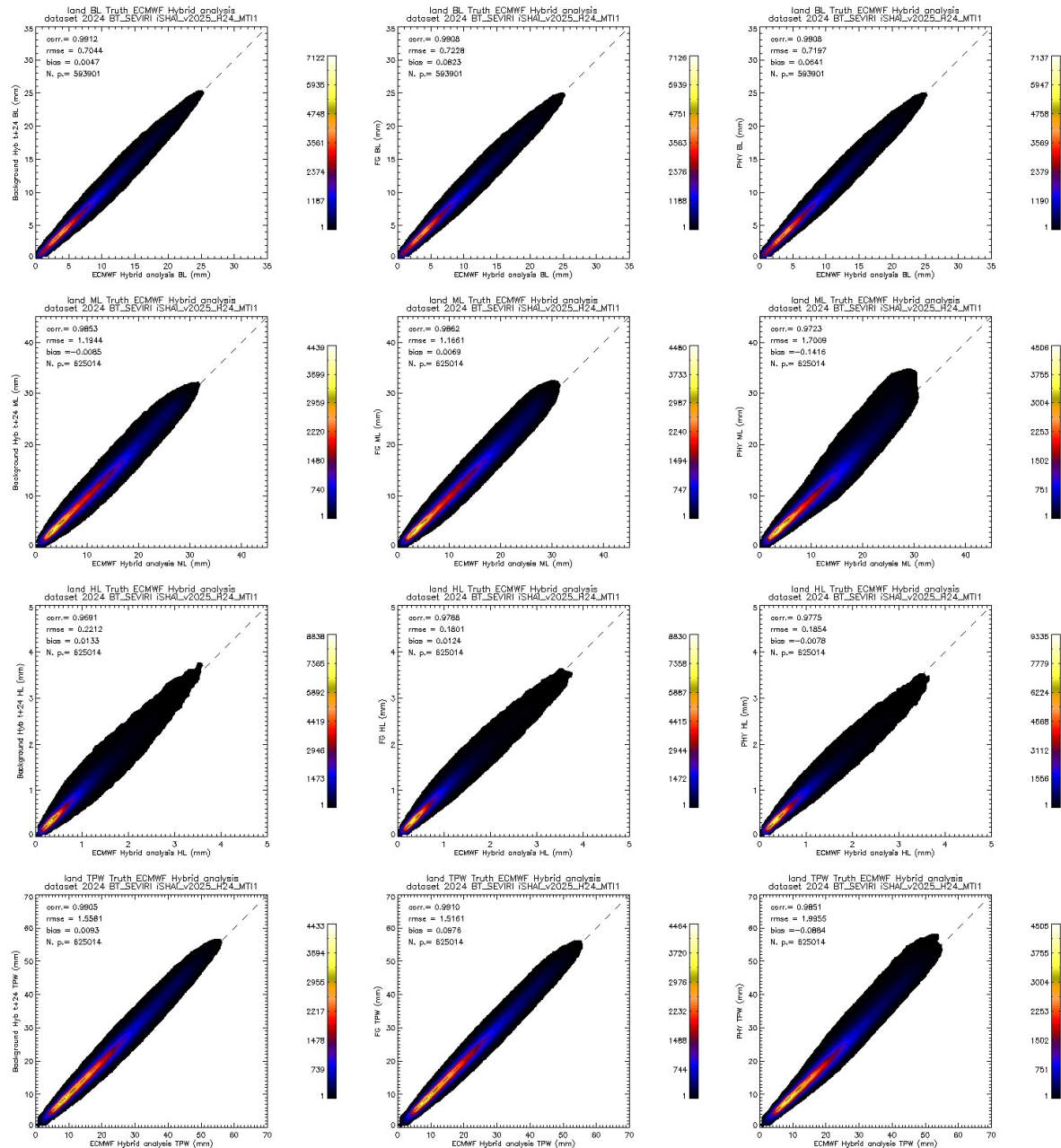


Figure 9: *Real_BT FCI MTII* case: LPW and TPW 2D histograms over *land* validation points. From top to bottom BL, ML, HL and TPW parameters. Left) Calculated directly from background ECMWF from hybrid profiles from (t+24) forecast, centre) Calculated after FG step profile using as input using real bias corrected SEVIRI BT, right) Calculated after physical retrieval step profile. In all case the ground truth are the BL, ML, HL and TPW calculated from Hybrid ECMWF analysis (t+00) profiles.

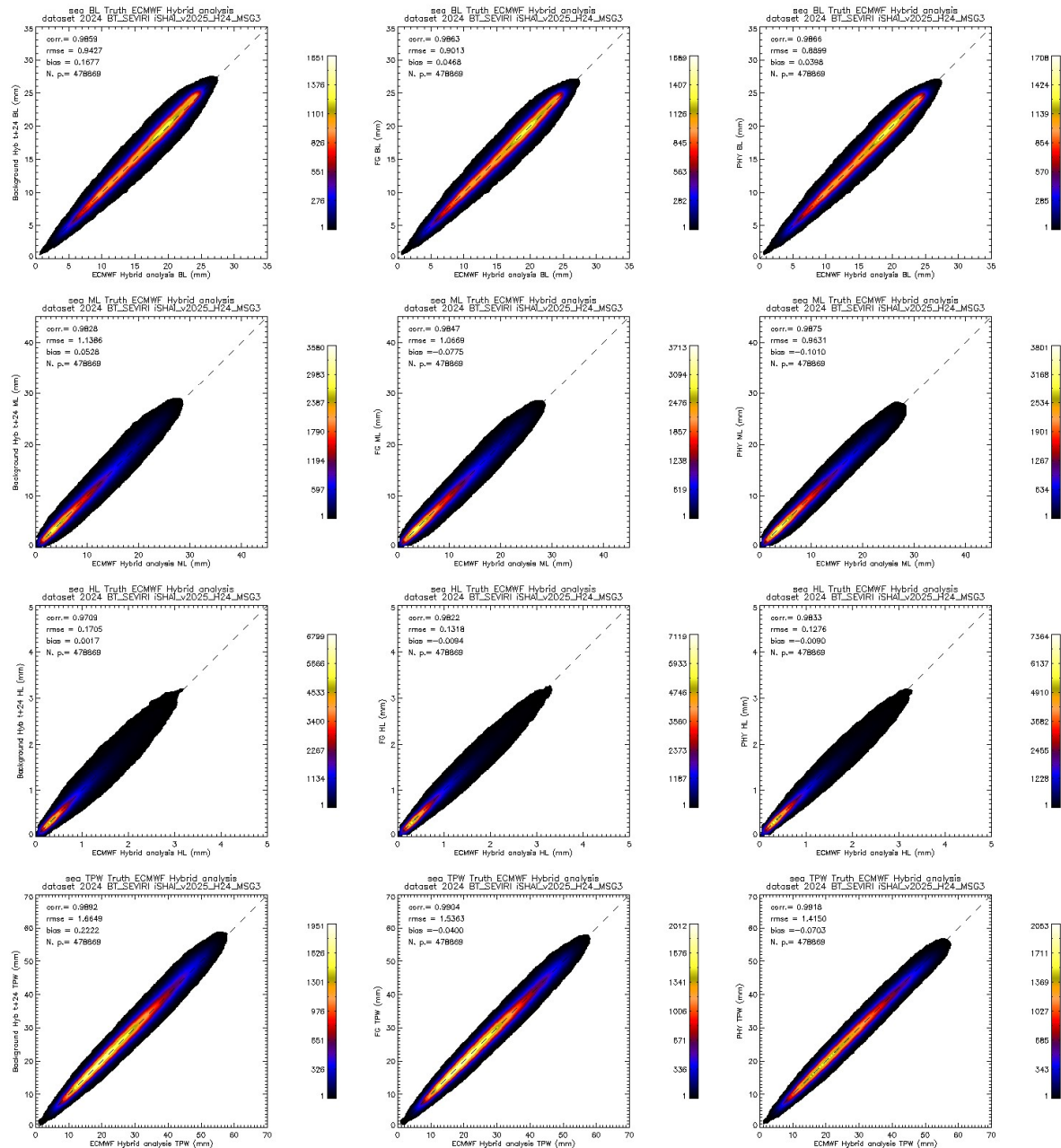


Figure 10: *Real_BT MSG3 case: LPW and TPW 2D histograms over sea validation points. From top to bottom BL, ML, HL and TPW parameters. Left) Calculated directly from background ECMWF from hybrid profiles from (t+24) forecast, centre) Calculated after FG step profile using as input using real bias corrected SEVIRI BT, right) Calculated after physical retrieval step profile. In all case the ground truth are the BL, ML, HL and TPW calculated from Hybrid ECMWF analysis(t+00) profiles.*

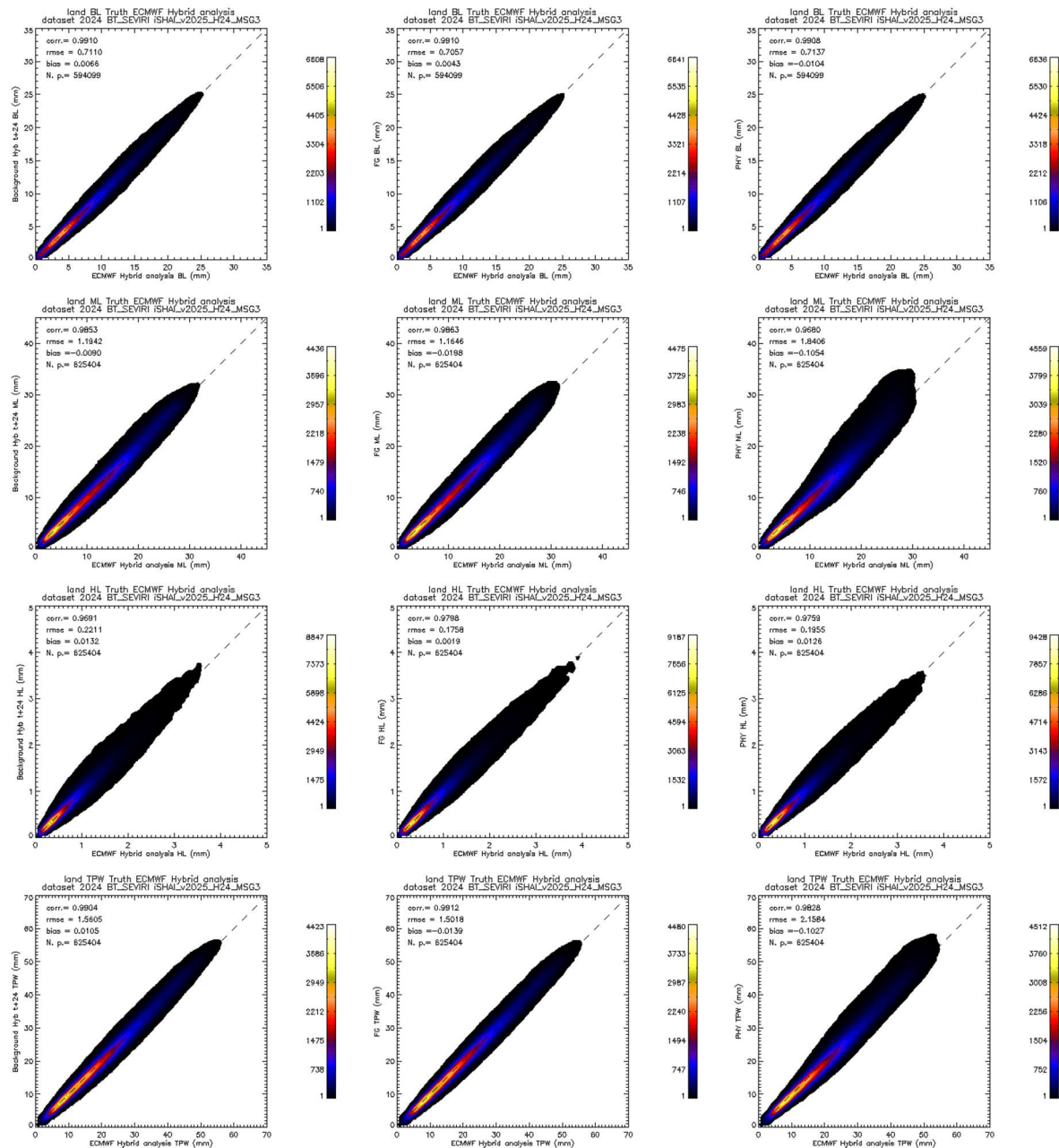


Figure 11: *Real_BT MSG3* case: LPW and TPW 2D histograms over *land* validation points. From top to bottom BL, ML, HL and TPW parameters. Left) Calculated directly from background ECMWF from hybrid profiles from (t+24) forecast, centre) Calculated after FG step profile using as input using real bias corrected SEVIRI BT, right) Calculated after physical retrieval step profile. In all case the ground truth are the BL, ML, HL and TPW calculated from Hybrid ECMWF analysis (t+00) profiles.

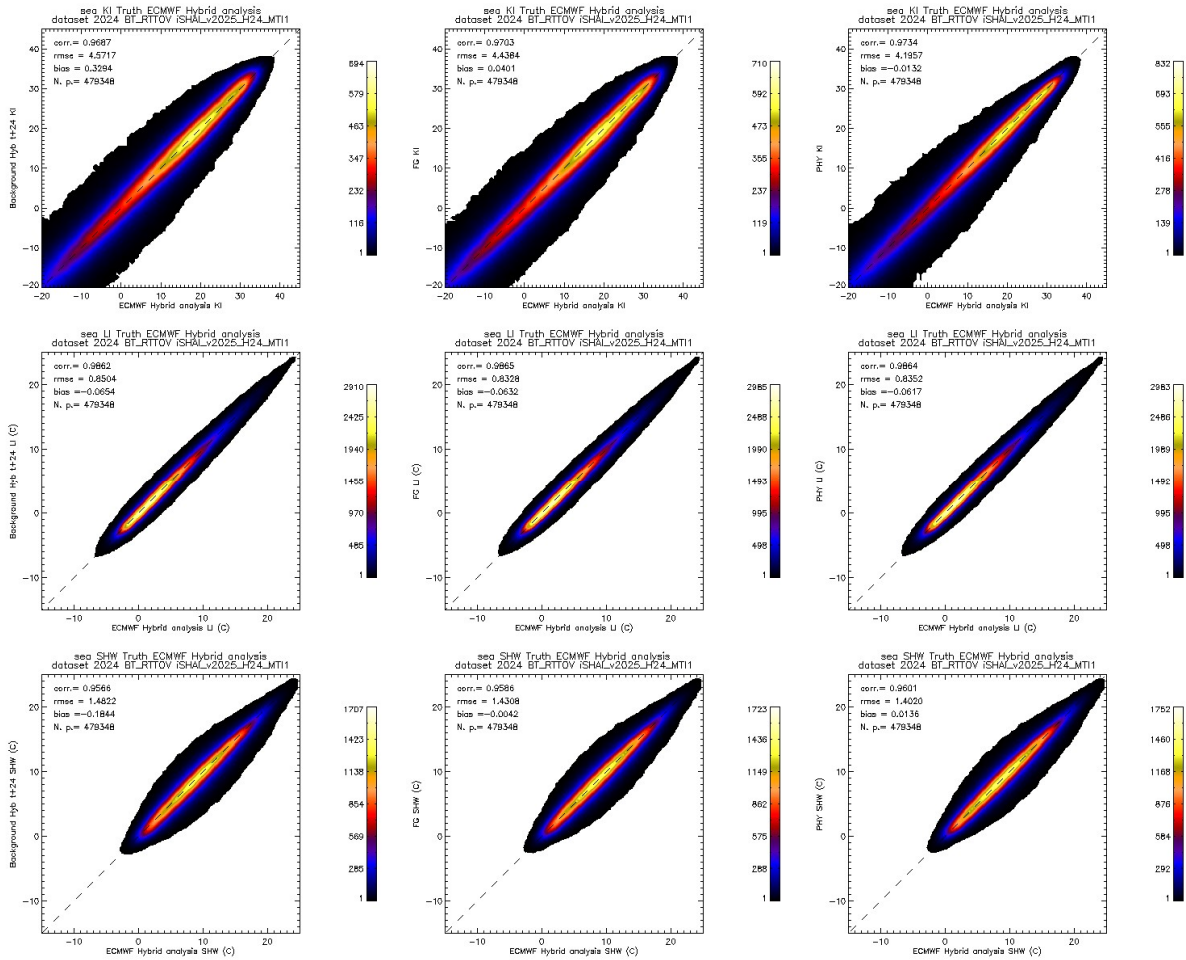


Figure 12: *BT_RTTOV FCI MTI1* case: instability indices 2D histograms over sea validation points. From top to bottom parameters KI, LI and SHW parameters. Left) calculated directly from background ECMWF from hybrid profiles from (t+24) forecast, centre) calculated after FG step profile using as input using real bias corrected SEVIRI BT, right) calculated after physical retrieval step profile. In all case the ground truth are the BL, ML, HL and TPW calculated from Hybrid ECMWF analysis (t+00) profiles.

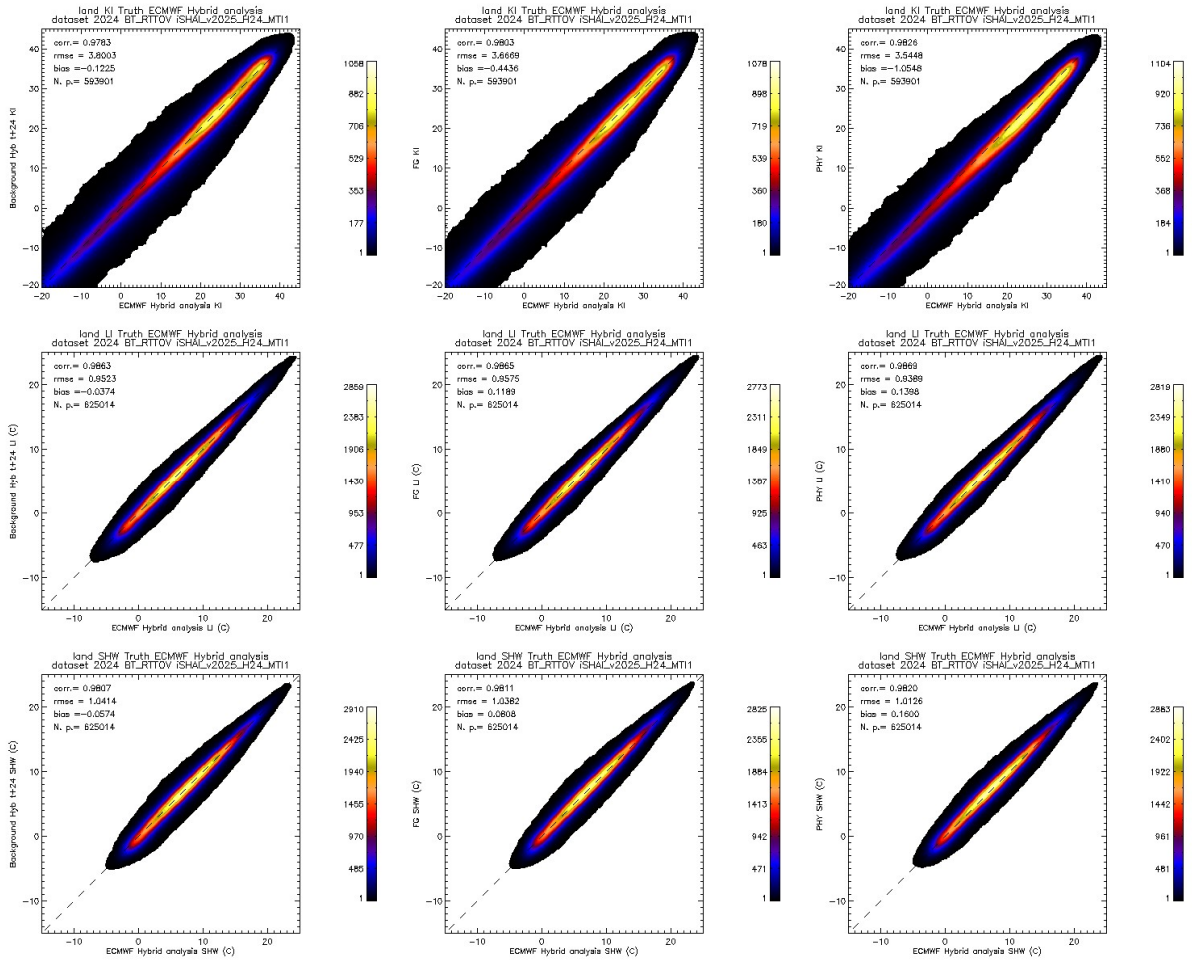


Figure 13: *BT_RTTOV FCI MTII* case: instability indices 2D histograms over *land* validation points. From top to bottom parameters KI, LI and SHW parameters. Left) calculated directly from background ECMWF from hybrid profiles from (t+24) forecast, centre) calculated after FG step profile using as input using real bias corrected SEVIRI BT, right) calculated after physical retrieval step profile. In all case the ground truth are the BL, ML, HL and TPW calculated from Hybrid ECMWF analysis (t+00) profiles.

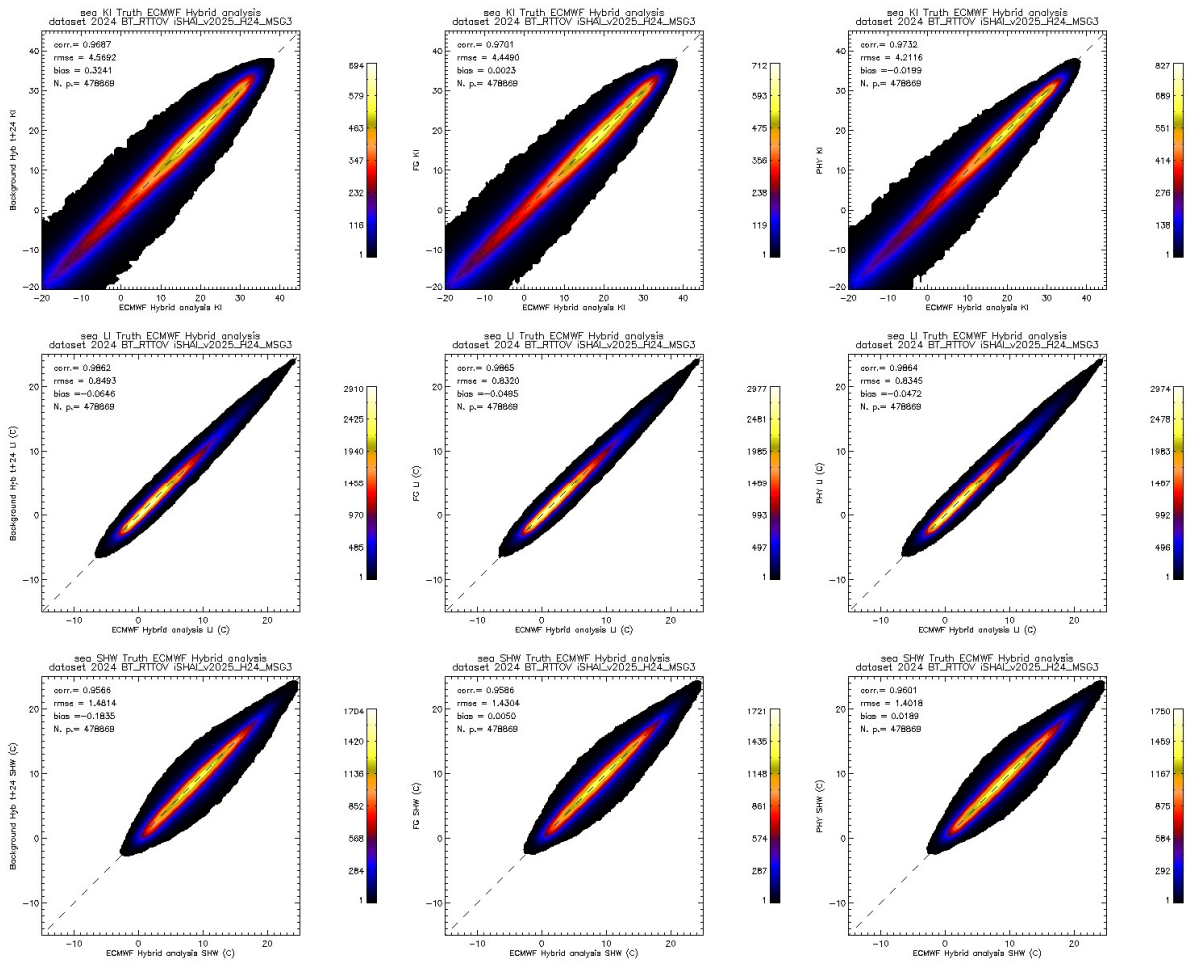


Figure 14: *BT_RTTOV MSG3* case: instability indices 2D histograms over *sea* validation points. From top to bottom parameters KI, LI and SHW parameters. Left) calculated directly from background ECMWF from hybrid profiles from (t+24) forecast, centre) calculated after FG step profile using as input using real bias corrected SEVIRI BT, right) calculated after physical retrieval step profile. In all case the ground truth are the BL, ML, HL and TPW calculated from Hybrid ECMWF analysis (t+00) profiles.

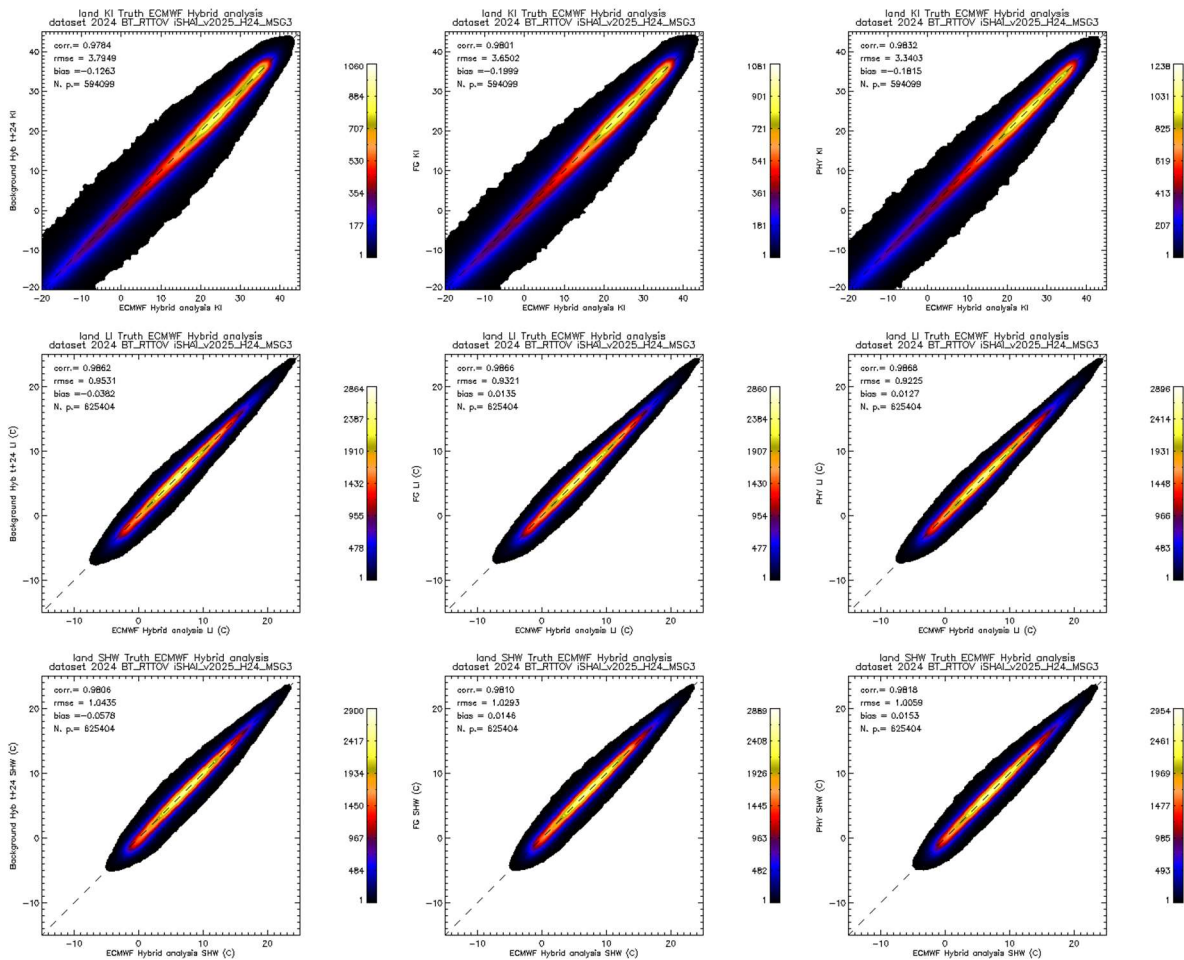


Figure 15: *BT_RTTOV MSG3* case: instability indices 2D histograms over *land* validation points. From top to bottom parameters KI, LI and SHW parameters. Left) calculated directly from background ECMWF from hybrid profiles from (t+24) forecast, centre) calculated after FG step profile using as input using real bias corrected SEVIRI BT, right) calculated after physical retrieval step profile. In all case the ground truth are the BL, ML, HL and TPW calculated from Hybrid ECMWF analysis (t+00) profiles.

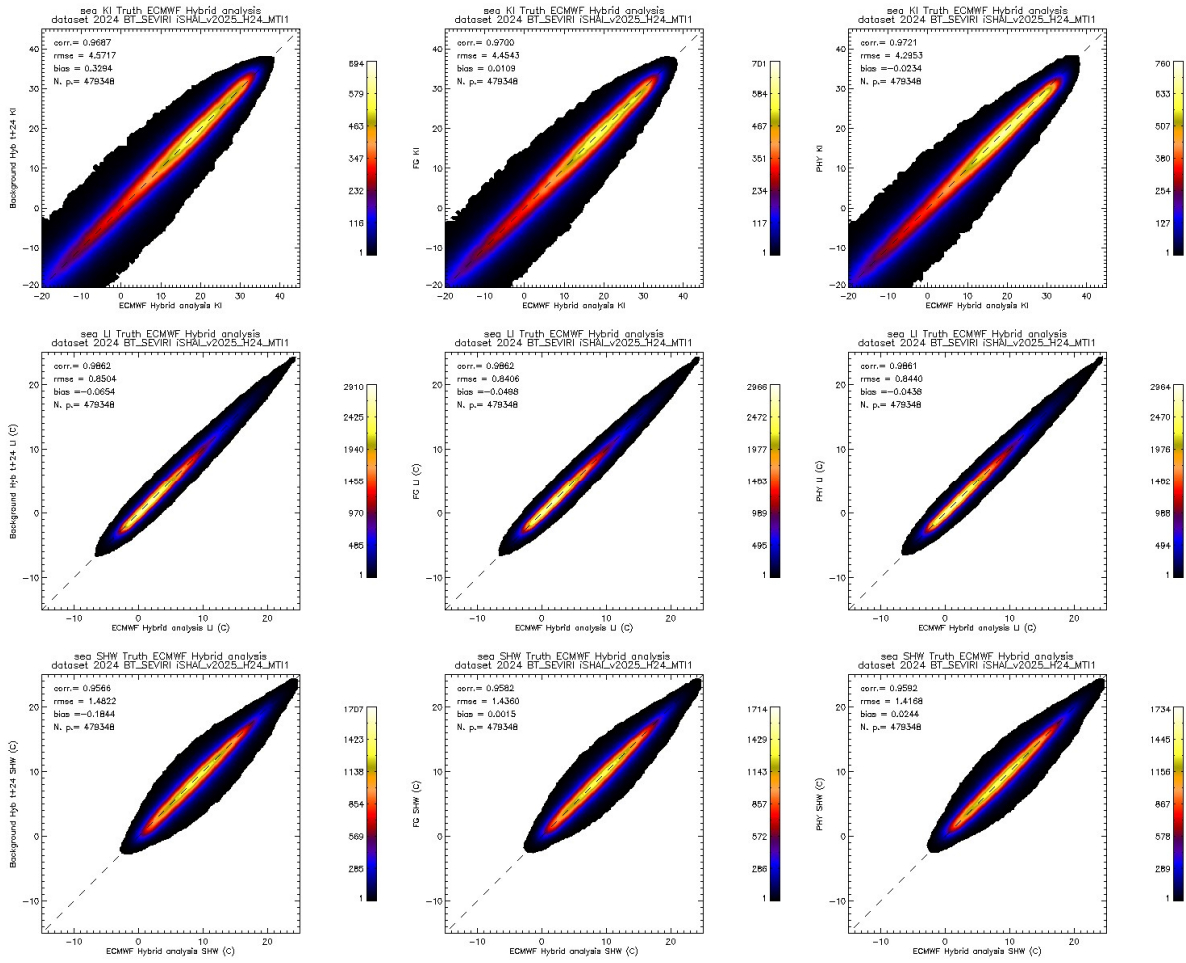


Figure 16: Real_BT FCI MTII case: instability indices 2D histograms over sea validation points. From top to bottom parameters KI, LI and SHW parameters. Left) calculated directly from background ECMWF from hybrid profiles from (t+24) forecast, centre) calculated after FG step profile using as input using real bias corrected SEVIRI BT, right) calculated after physical retrieval step profile. In all case the ground truth are the BL, ML, HL and TPW calculated from Hybrid ECMWF analysis (t+00) profiles.

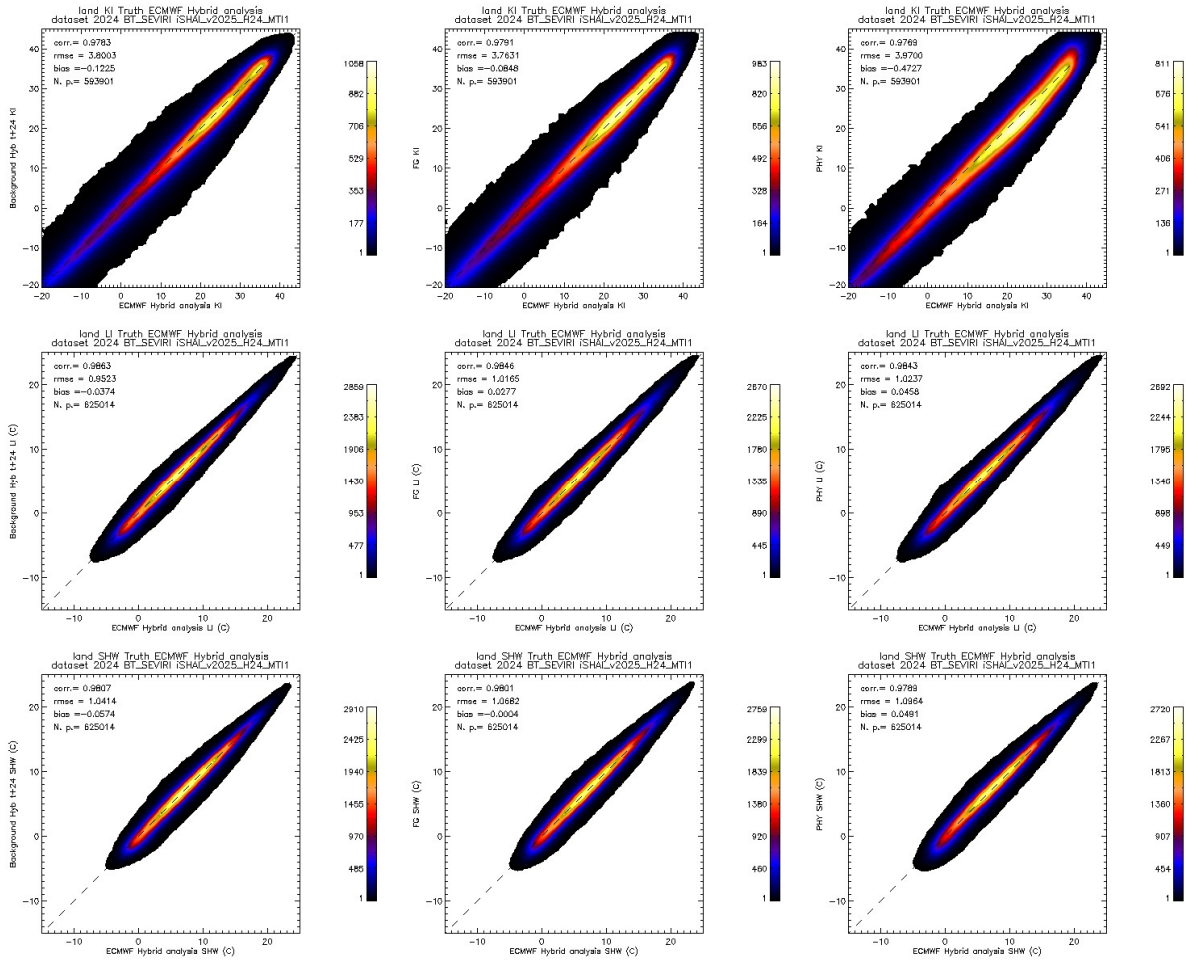


Figure 17: Real_BT FCI MTI1 case: instability indices 2D histograms over land validation points. From top to bottom parameters KI, LI and SHW parameters. Left) calculated directly from background ECMWF from hybrid profiles from (t+24) forecast, centre) calculated after FG step profile using as input using real bias corrected SEVIRI BT, right) calculated after physical retrieval step profile. In all case the ground truth are the BL, ML, HL and TPW calculated from Hybrid ECMWF analysis (t+00) profiles.

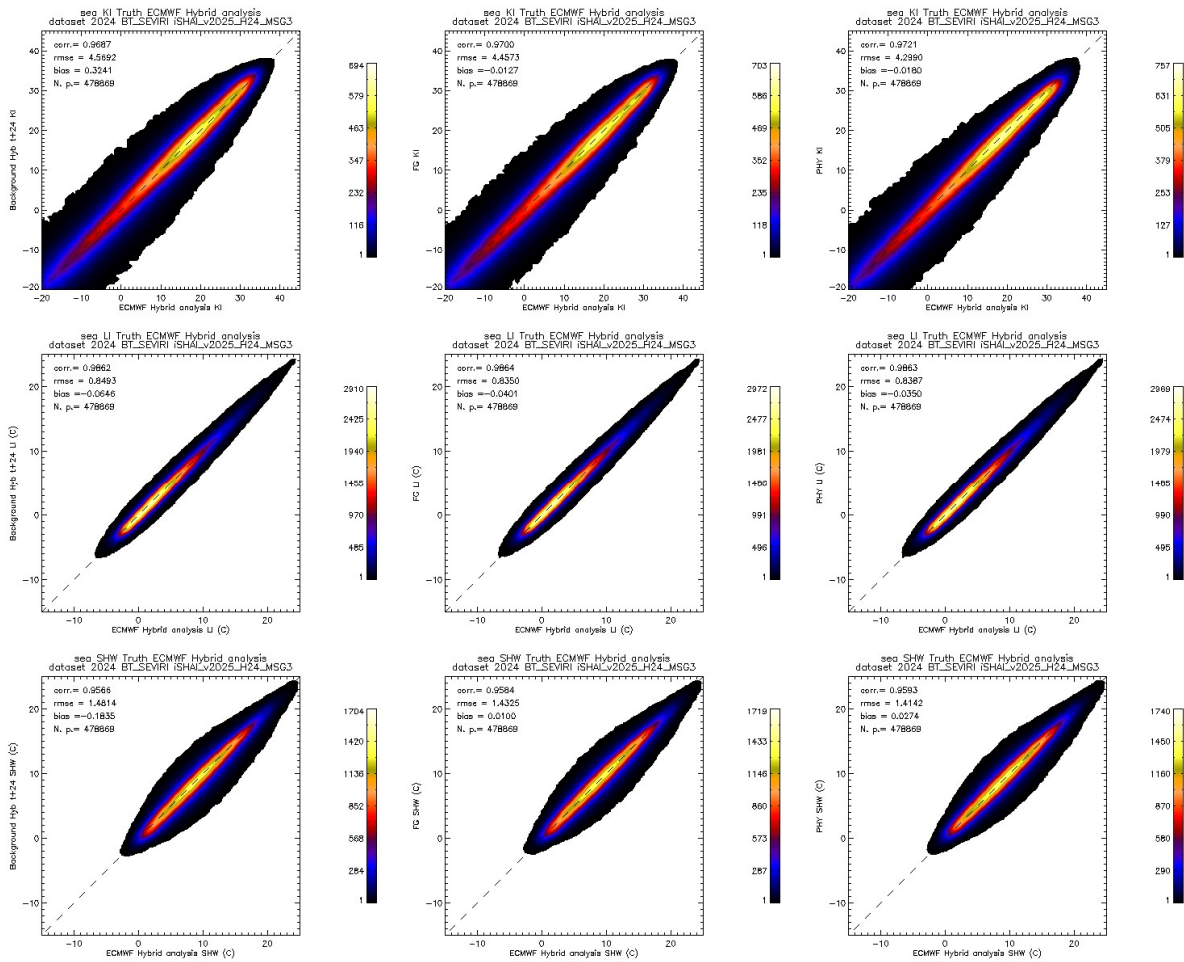


Figure 18: **Real_BT MSG3** case: instability indices 2D histograms over **sea** validation points. From top to bottom parameters KI, LI and SHW parameters. Left) calculated directly from background ECMWF from hybrid profiles from (t+24) forecast, centre) calculated after FG step profile using as input using real bias corrected SEVIRI BT, right) calculated after physical retrieval step profile. In all case the ground truth are the BL, ML, HL and TPW calculated from Hybrid ECMWF analysis (t+00) profiles.

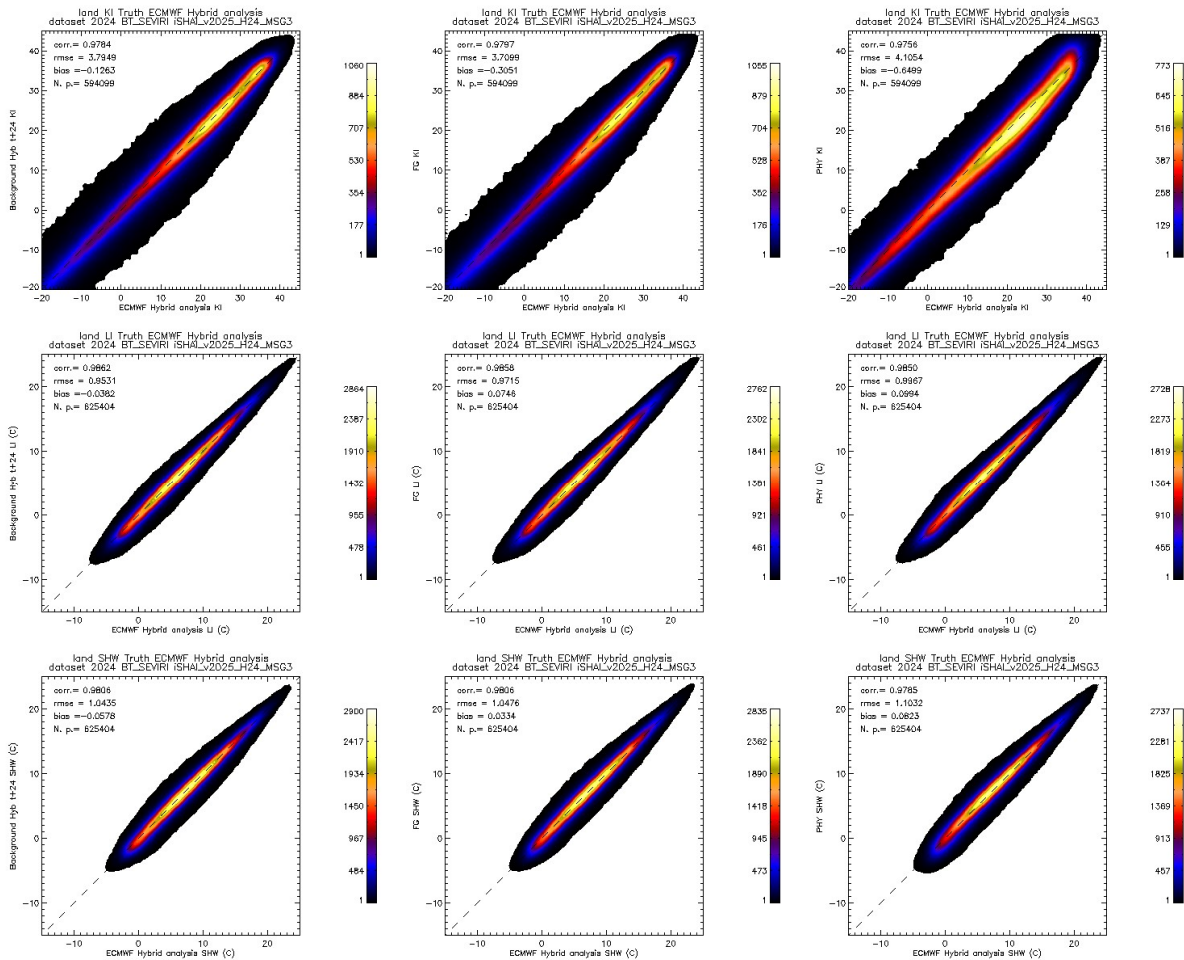


Figure 19: Real_BT MSG3 case: instability indices 2D histograms over *land* validation points.
From top to bottom parameters KI, LI and SHW parameters. Left) calculated directly from background ECMWF from hybrid profiles from (t+24) forecast, centre) calculated after FG step profile using as input using real bias corrected SEVIRI BT, right) calculated after physical retrieval step profile. In all case the ground truth are the BL, ML, HL and TPW calculated from Hybrid ECMWF analysis (t+00) profiles.

3.2 SPATIAL ANALYSIS OF GEO ISHAI PARAMETERS

In the Figures on this Section the spatial performance of the iSHAI parameters for BT_RTTOV case and Real_BT cases and for both FCI and SEVIRI instruments are shown. From the comparison of spatial RMSE and the spatial relative_RMSE it can be seen that for LPWs and TPW parameter some regions with high RMSE are not so bad and the high value of RMSE is linked to higher amount of precipitable water (the tropical forest at Equatorial regions) than in other colder and dryer regions. Other regions with higher than mean RMSE are desert regions due to combination of large errors in fixed emissivity atlases and the greater differences between NWP SKT and real SKT.

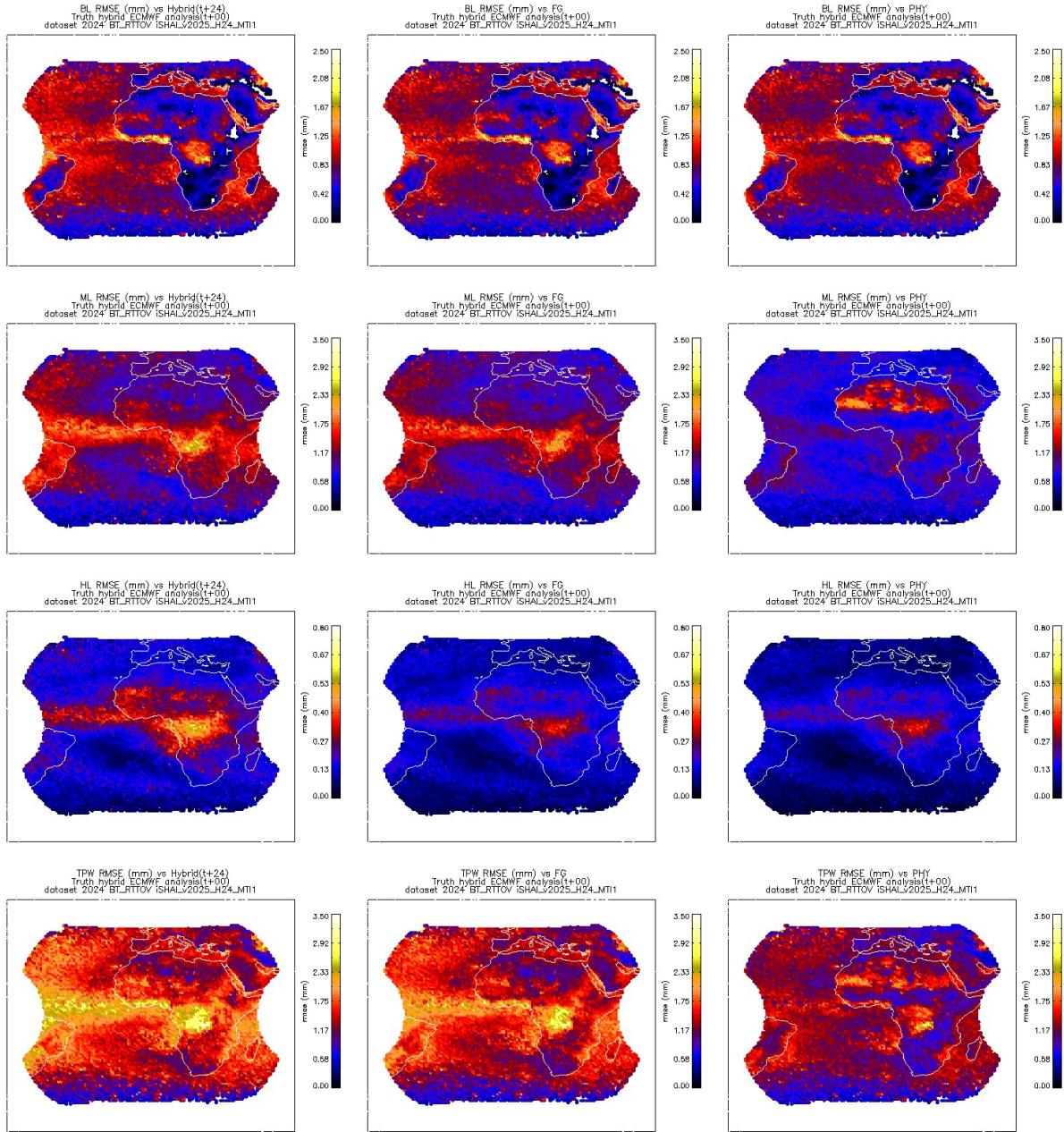
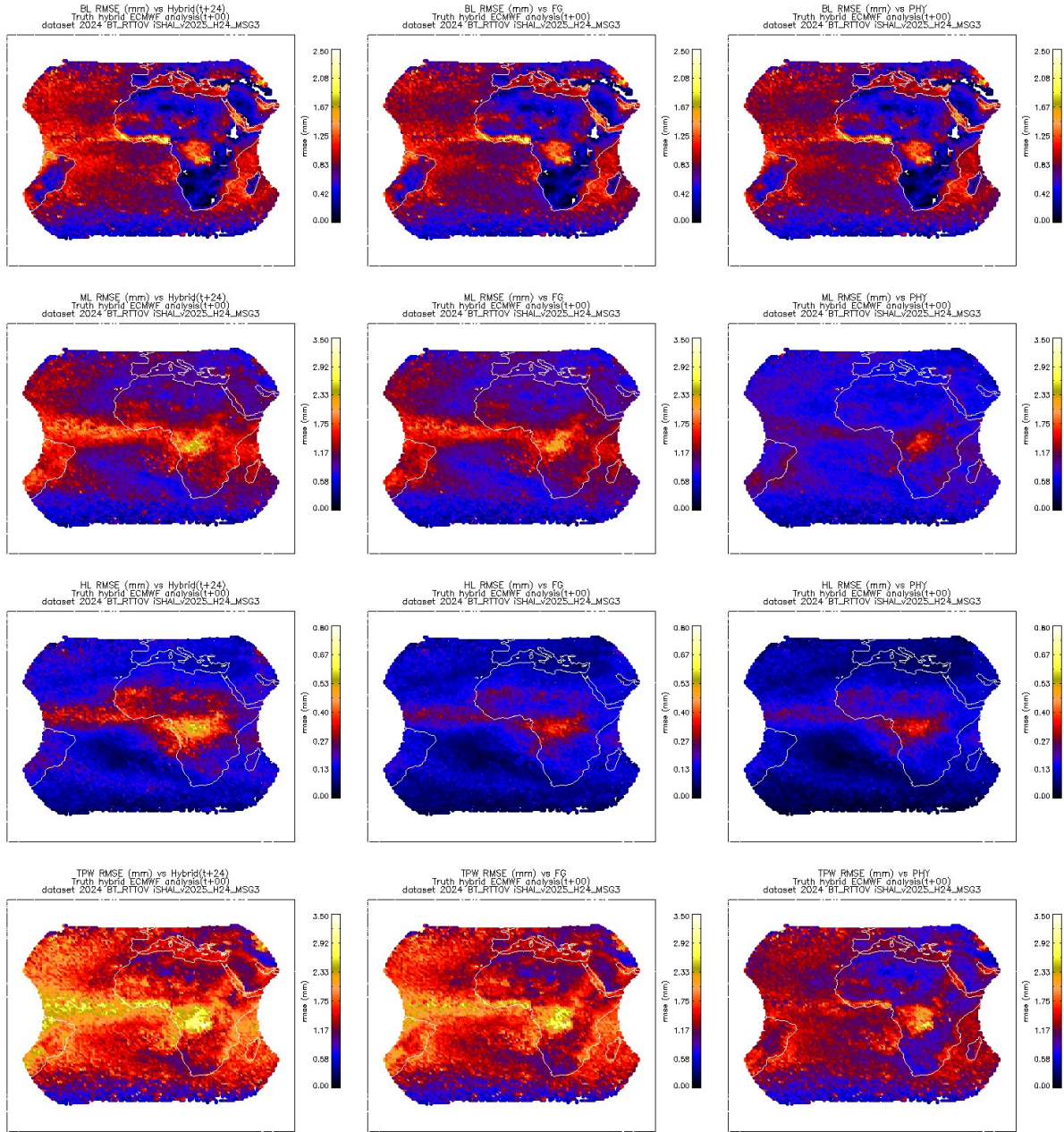


Figure 20: *BT_RTTOV FCI MTI* case: Spatial distribution of the BL, ML, HL and TPW RMSE over validation points. From top to bottom BL, ML, HL and TPW parameters. Left) BL, ML, HL and TPW RMSE calculated directly from background ECMWF hybrid GRIB (t+24), centre) BL, ML, HL and TPW RMSE calculated after FG step profile, right) BL, ML, HL and TPW RMSE calculated after physical retrieval step profile. In all case the ground truth are the BL, ML, HL and TPW calculated from NWP-Hyb ECMWF analysis (t+00) profiles.



*Figure 21: **BT_RTTOV MSG3** case: Spatial distribution of the BL, ML, HL and TPW RMSE over validation points. From top to bottom BL, ML, HL and TPW parameters. Left) BL, ML, HL and TPW RMSE calculated directly from background ECMWF hybrid GRIB (t+24), centre) BL, ML, HL and TPW RMSE calculated after FG step profile, right) BL, ML, HL and TPW RMSE calculated after physical retrieval step profile. In all case the ground truth are the BL, ML, HL and TPW calculated from NWP-Hyb ECMWF analysis (t+00) profiles.*

The greatest values of ML and HL RMSE appear near the equatorial belt. But, when the relative ML RMSE are calculated, this effect disappears due to the high amount of precipitable water close to the equatorial belt. This effect can be seen in next Figures.

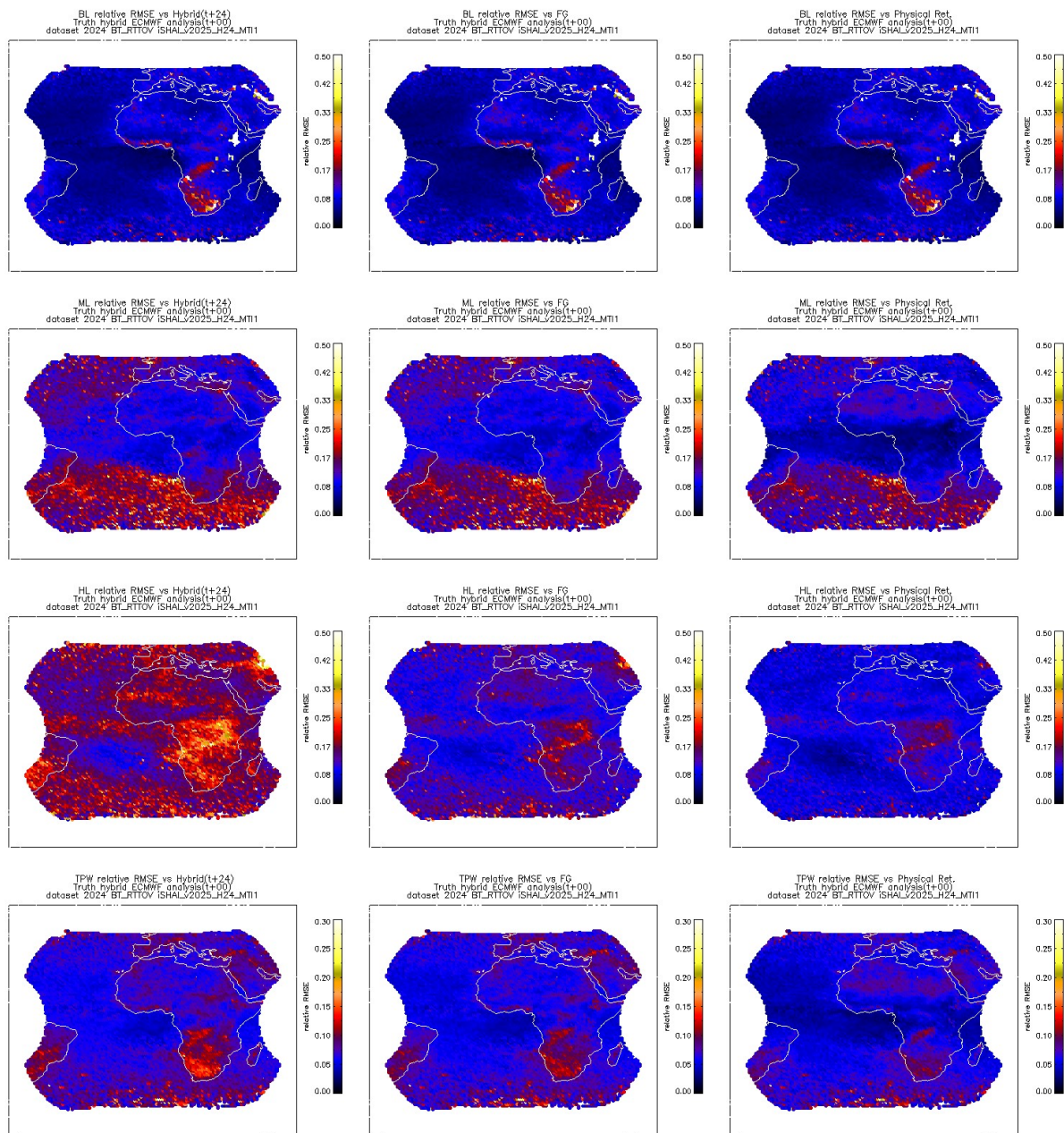


Figure 22: *BT_RTOV FCI MTI1 case: Same that Figure 20 but relative RMSE instead of RMSE.*

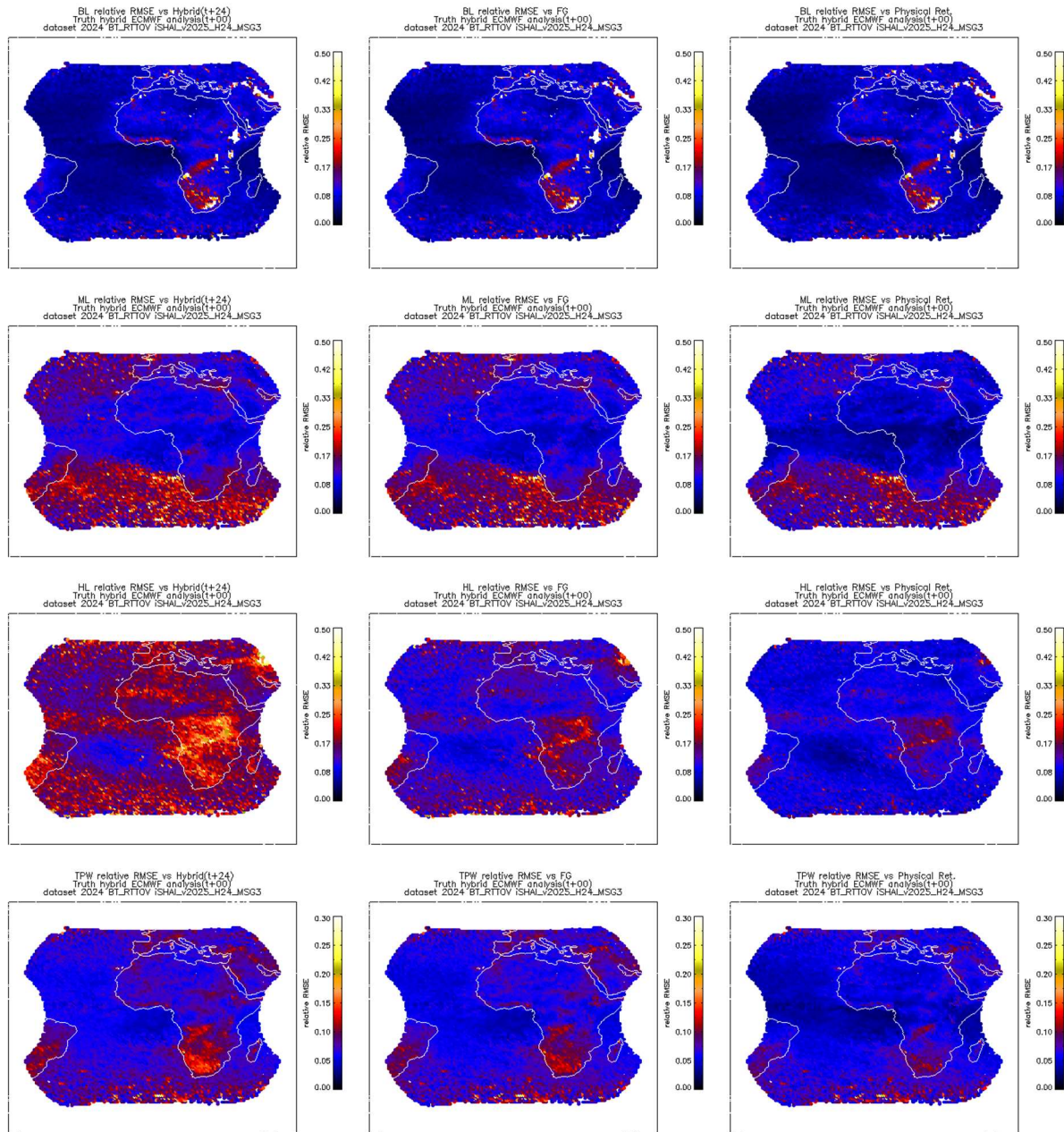


Figure 23: BT_RTTOV MSG3 case: Same that Figure 21 but relative RMSE instead of RMSE.

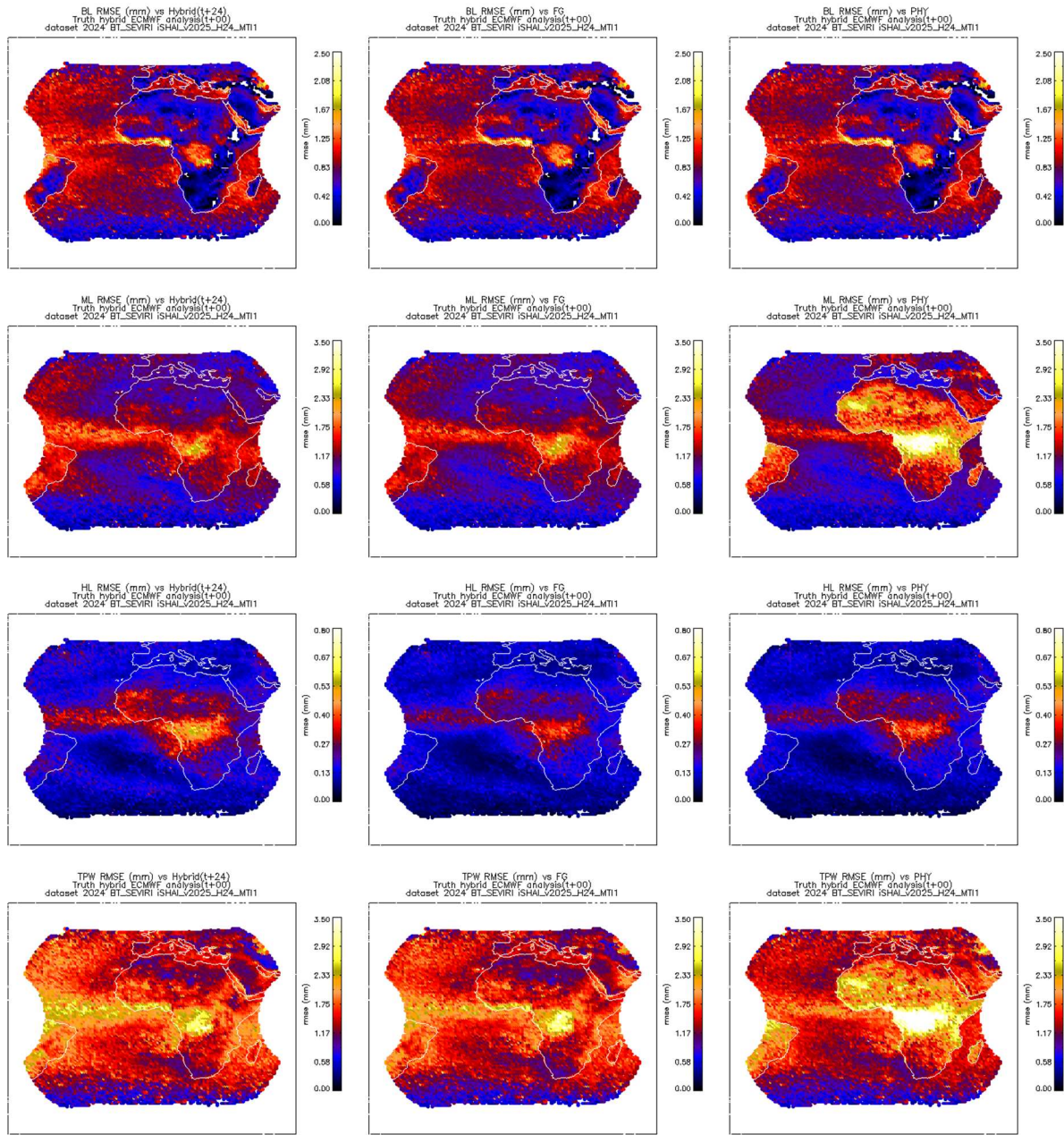


Figure 24: Real_BT FCI MTI case: Spatial distribution of the BL, ML, HL and TPW RMSE over validation points. From top to bottom BL, ML, HL and TPW parameters. Left) BL, ML, HL and TPW RMSE calculated directly from background ECMWF hybrid GRIB (t+24), centre) BL, ML, HL and TPW RMSE calculated after FG step profile, right) BL, ML, HL and TPW RMSE calculated after physical retrieval step profile. In all case the ground truth are the BL, ML, HL and TPW calculated from NWPhyb ECMWF analysis(t+00) profiles.

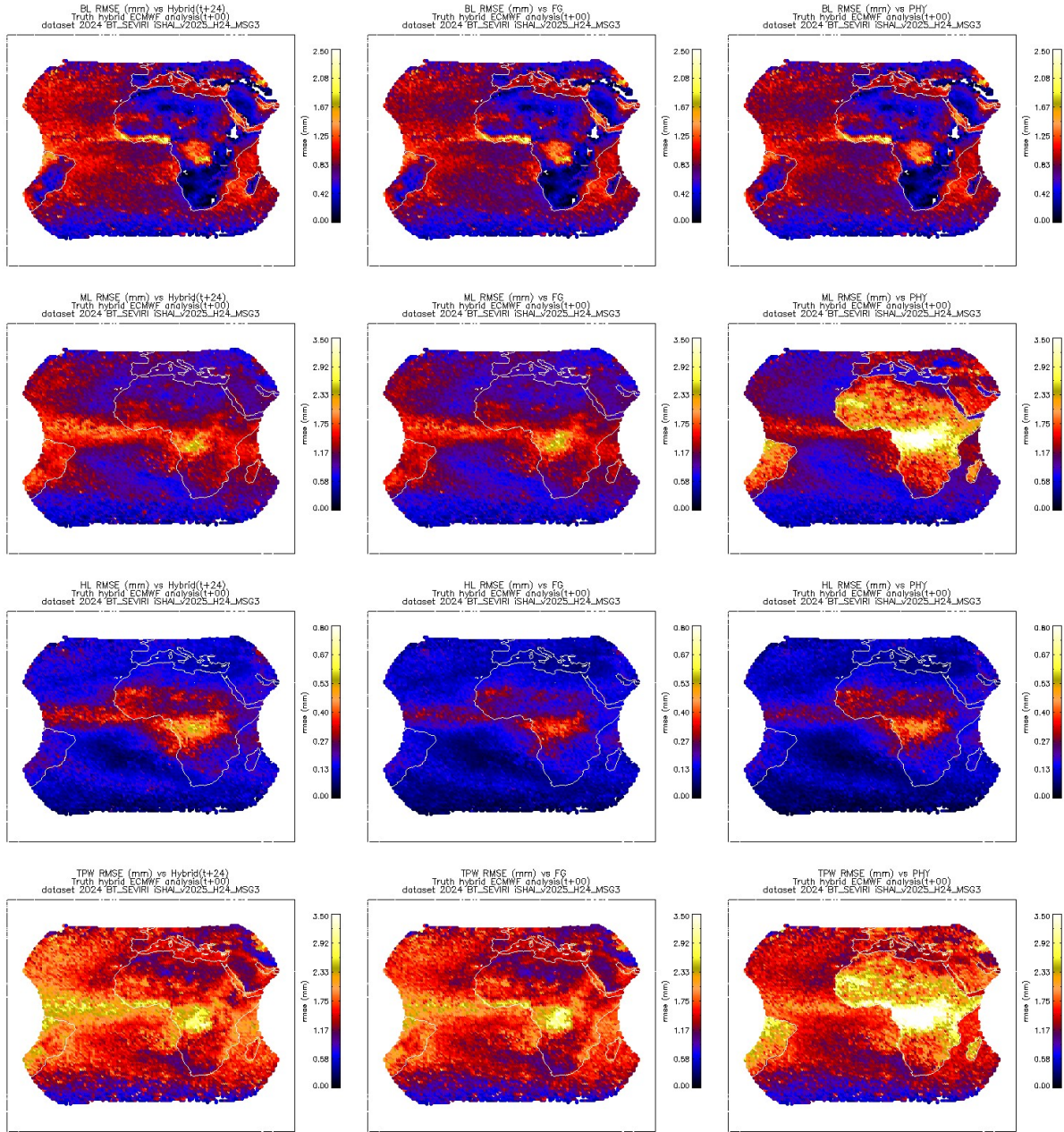


Figure 25: Real_BT MSG3 case: Spatial distribution of the BL, ML, HL and TPW RMSE over validation points. From top to bottom BL, ML, HL and TPW parameters. Left) BL, ML, HL and TPW RMSE calculated directly from background ECMWF hybrid GRIB (t+24), centre) BL, ML, HL and TPW RMSE calculated after FG step profile, right) BL, ML, HL and TPW RMSE calculated after physical retrieval step profile. In all case the ground truth are the BL, ML, HL and TPW calculated from NWPhyb ECMWF analysis(t+00) profiles.

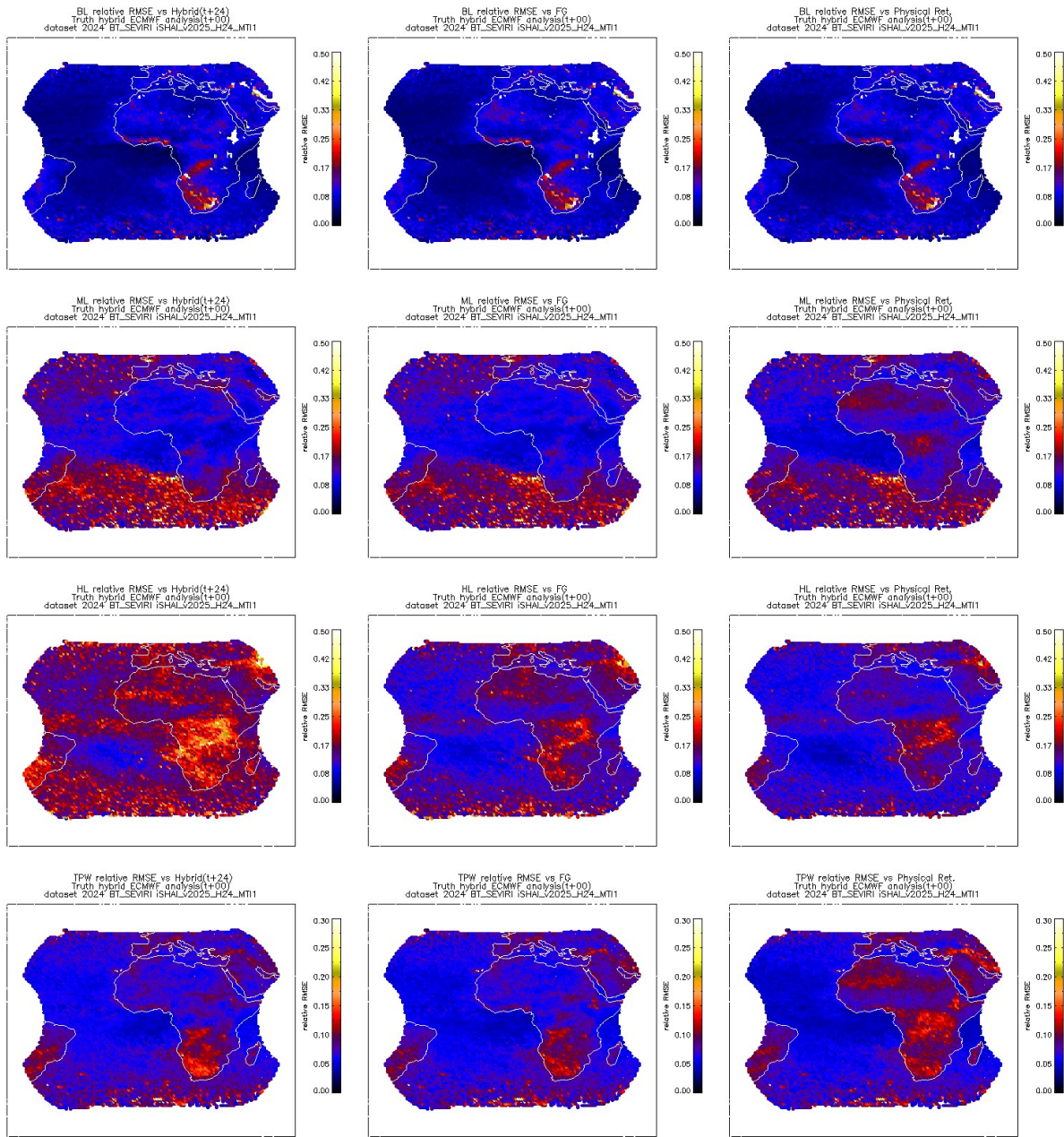


Figure 26: *Real_BT FCI MTI1 case: Same that Figure 24 but relative RMSE instead of RMSE.*

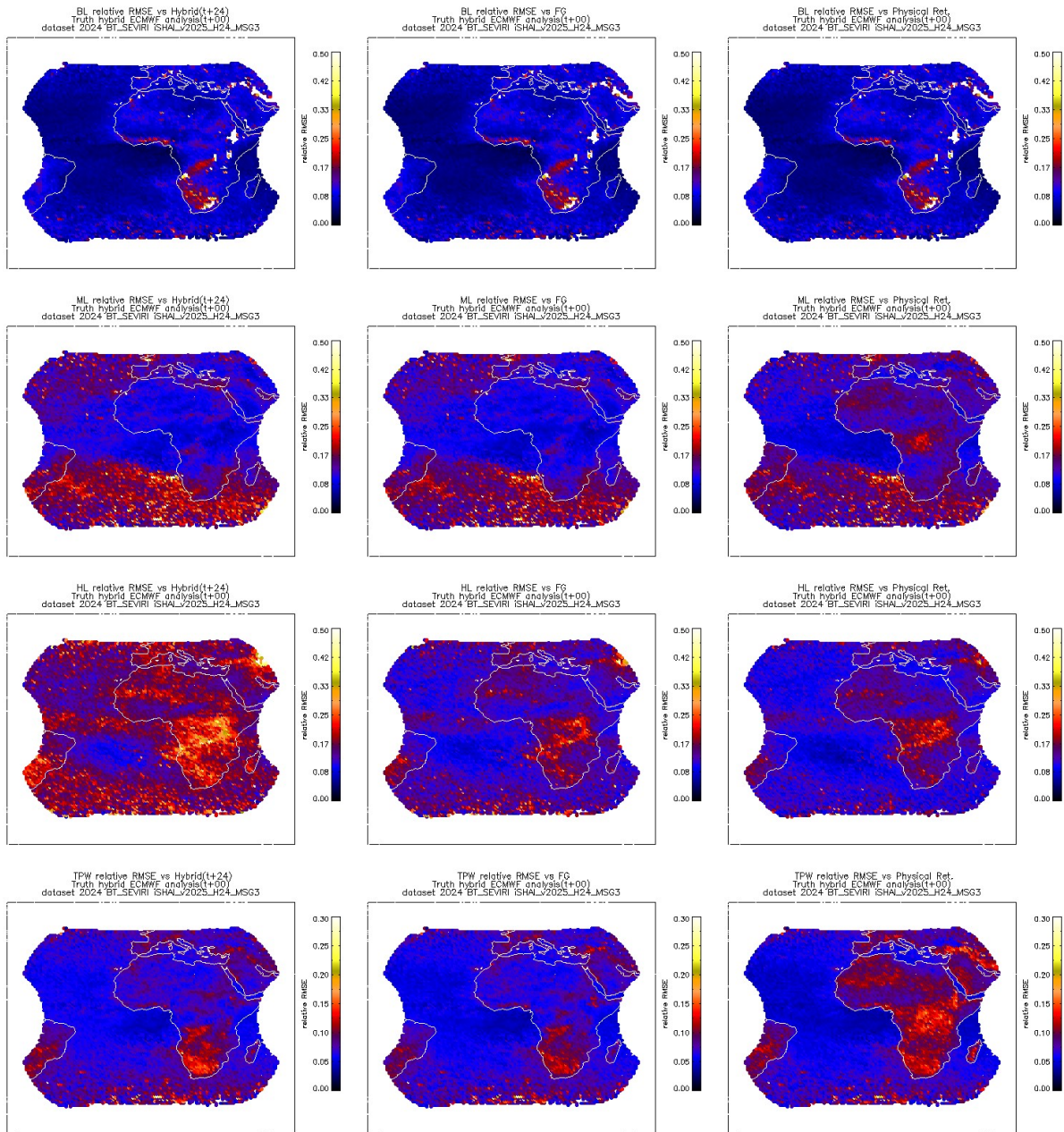
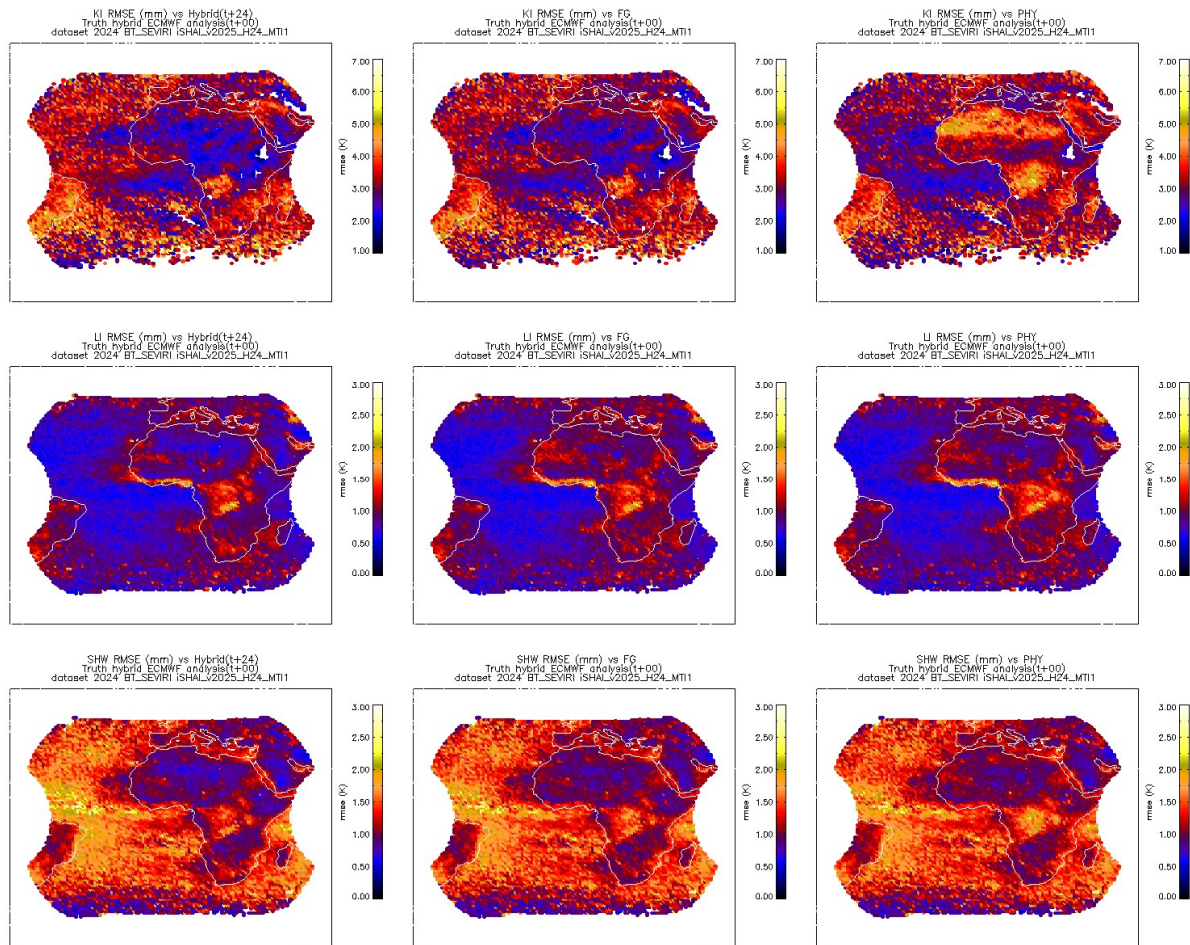


Figure 27: Real_BT MSG3 case: Same that Figure 25 but relative RMSE instead of RMSE.



*Figure 28: **Real_BT FCI MTI1 case:** Spatial distribution of the KI, LI and SHW RMSE over validation points. From top to bottom KI, LI and SHW parameters. Left) RMSE calculated directly from background ECMWF hybrid GRIB (t+24), centre) RMSE calculated after FG step profile, right) RMSE calculated after physical retrieval step profile. In all case the ground truth are the KI, LI and SHW calculated from NWPHyb ECMWF analysis(t+00) profiles.*

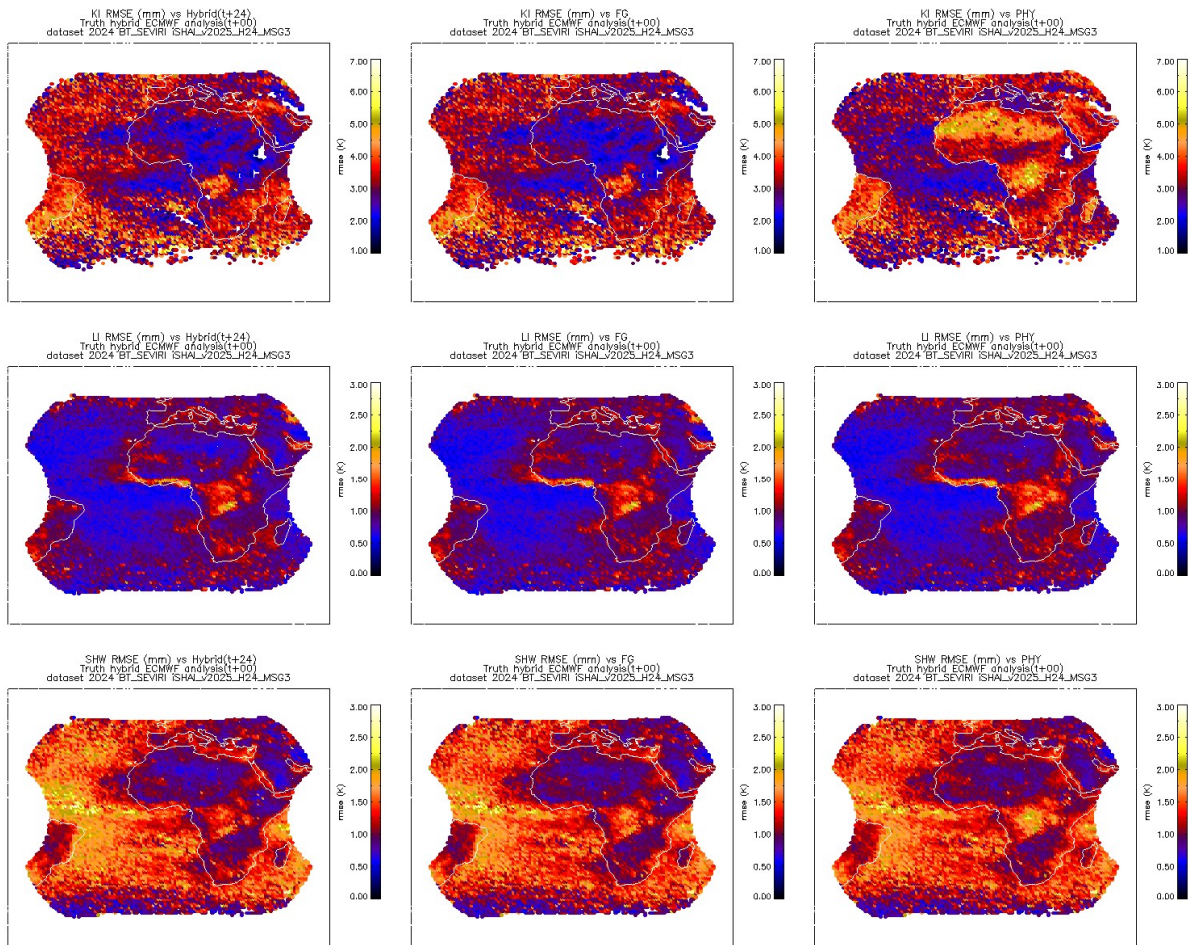


Figure 29: Real_BT MSG3 case: Spatial distribution of the KI, LI and SHW RMSE over validation points. From top to bottom KI, LI and SHW parameters. Left) RMSE calculated directly from background ECMWF hybrid GRIB (t+24), centre) RMSE calculated after FG step profile, right) RMSE calculated after physical retrieval step profile. In all case the ground truth are the KI, LI and SHW calculated from NWPHyb ECMWF analysis(t+00) profiles.

3.3 SUMMARY OF LPW AND STABILITY INDICES PERFORMANCES

The iSHAI validation results are similar for FCI MTI1 and SEVIRI MSG-3.

GEO-iSHAI validation with real bias BT corrected FCI or SEVIRI BTs the performance has the same behaviour that synthetic RTTOV ones but with higher figures and irregular distribution of the RMSE; especially over the land pixels.

ML parameter shows a significant theoretical reduction in RMSE with GEO-iSHAI. From the values on the 2D histograms, it can be seen the greatest reduction in ML RMSE % for FG step and after physical retrieval.

It should be remembered that these values have been obtained after the screening to remove the pixels with largest BT_RMS . If a perfect screening would be possible and a real truth could be obtained, then the performance would tend to the theoretical reduction in RMSE for the BT_RTTOV case. As in the analysis of previous statistical values, the combinations of several sources of errors and uncertainties over land are a potential reason to explain the worse performance of ML over land.

In the case of HL parameter the percentage in the reduction with GEO-iSHAI are also high. This better performance of HL parameter confirms that the WV channels have the greatest contribution and the source of errors as emissivity uncertainties and skin temperature affect less the HL parameter.

In the case of the stability indices, there is less clear statistical reduction in the RMSE with GEO iSHAI. Looking at values for the BT_RTTOV case, the performance is better for the stability indices which involve the lower level at 850 hPa (Showalter Index and KI). Likely, this is due to the fact that FCI and SEVIRI have limited information to improve the temperature vertical information beyond the forecast. This fact is also explained from the vertical analysis of section 3.4; the highest reduction on q RMSE is on middle and high levels due to WV channels. Thus, it would be advisable to start looking for optimal stability indices from satellite retrievals of temperature and humidity profiles.

But although the statistical validation is not much better, the GEO-iSHAI stability indices have a great added value because SEVIRI provides useful spatial and temporal resolution. It is important to take into account that a certain degree of disagreement between ECMWF analysis and real temperature and humidity profiles always exists. In CDOP-5 the availability of MTG-S/IRS L2 could be a good truth for training and validation. For this reason, this is not always a negative aspect that the statistical values in real BT case are greater than the ones in BT_RTTOV case because it reflects the fact that real BT s from the real world are not the same that the synthetic and ideal RTTOV BT s ($t+00$). One of the added values of the GEO-iSHAI is to show where and when there is a disagreement between ECMWF forecast or analysis against the real bias corrected BT s retrieved profiles. Thus, the GEO-iSHAI stability parameters are able to delimitate the region where instability is growing before convection is triggered, as it can be seen on the study case loops or in the near real time loops in <http://nwc-saf.eumetsat.int>.

It is needed to repeat with wider period dataset the comparison of 2D histograms over several regions with the one from the full disc. In Validation Reports from previous version there were a big differences on 2D histograms on Europe region with the ones from the full disc (see Validation Report for version 2018). It was shown that the spread up in 2D histograms over land was caused mainly by the Sahara desert and the tropical forest at Equatorial regions.

3.4 ANALYSIS OF THE PERFORMANCE AT DIFFERENT VERTICAL LEVELS

In the Figures on this section, the RMSEs between the q profiles after several steps in the GEO iSHAI for the full disc dataset at the 54 RTTOV levels have been represented.

The profiles of the ECMWF analysis ($t+00$) from NWP-Hyb datasets (137 hybrid levels interpolated to the 54 RTTOV level) have been considered as the truth.

The statistical values for the specific humidity at mid-levels show better performance for the FG regression and the FG+physical retrieval steps than the background NWP model (ECMWF GRIB files on hybrid levels from $t+24$ forecast). This is likely due to the added value of the WV channels on FCI or SEVIRI, the reduction in the RMSE at these levels indicates that the GEO iSHAI slightly improves the q profile from background NWP.

The performance is better over sea pixels. The worse performance over land can be due to a combination of all sources of errors that can affect the calculation of the synthetic BT (uncertainties in the emissivity atlas, errors due to contamination with clouds on some pixels (not well filtered by the Cloud Mask), errors in the radiative transfer model RTTOV, noise of real SEVIRI image, etc.)

Several experiments with previous PGE13 and iSHAI versions, not shown here, to compare the GEO iSHAI performance with some modifications were made. The first experiment was to suppress the FG regression step and use directly as First Guess the $t+24$ forecast profiles from ECMWF GRIB files on hybrid levels; but the performance of GEO iSHAI with FG regression step was slightly better.

These experiments and the faster executions of GEO iSHAI with FG regression step (avoiding the execution of the physical retrieval step on all clear FOR) have inclined us to maintain the FG regression step on the GEO iSHAI algorithm. Hereafter, in the figures the meaning of the labels is the following:

1. **Hybrid $t+24$:** indicates that the value has been calculated using the comparison of ECMWF $t+24$ forecast and the ECMWF analysis $t+00$ as truth.
2. **FG:** indicates that the value has been calculated using comparison of the result to execute the non-linear regressions of FG step over the satellite BTs case and the ECMWF $t+24$ forecast and the ECMWF analysis $t+00$ as truth.
3. **PHY:** indicates that the value has been calculated using comparison of the result to execute the non-linear regressions of FG step followed by the physical retrieval step over the satellite BTs case and the ECMWF $t+24$ forecast and the ECMWF analysis $t+00$ as truth.

It can be seen in previous Validation Reports (2012) that the use of ECMWF with only 15 fixed pressure levels profiles as input to the PGE13 SPhR created several “peaks” and irregularities in the RMSE and bias vertical distribution centred at the 15 fixed pressure levels. This was another reason to strongly recommend the use of GRIB files with the maximum number of vertical levels as possible as the background NWP input to GEO iSHAI. For this reason the performance of GEO iSHAI processor with GRIB files on hybrid levels as background NWP input is the best possible.

The NWC/GEO package versions 2025 will continue with the use of the fixed pressure levels as background NWP input to GEO iSHAI, since the 2025 version of NWC SAF library only allows reading GRIB files on fixed pressure. GEO-iSHAI is just one advance of future versions of NWC/GEO processing. The details to activate GEO-iSHAI on hybrid levels instead to the regular GEO iSHAI on P levels can be found in the GEO-iSHAI User Manual [RD.2].

In order to show that the source of the increase of q rmse on land SEVIRI case is associated to some regions it will be repeated with a wider period some validation tests made in previous versions to calculate all the figures in this Validation Report for some regions. In previous Validation Report one was European latitudes region (considered as latitude greater than 36 °N) and the results were one strong reduction in q rmse in the land SEVIRI case in the layer 900-600 hPa; due to the profiles from tropical forest and Sahara desert was excluded.

It can be seen in the Figures of this Section a reduction in the RMSE and an improvement over the background NWP in the q profile at middle levels. The reduction of RMSE in the middle levels of the q profile is likely the main contribution for the reduction in the ML and TPW RMSE.

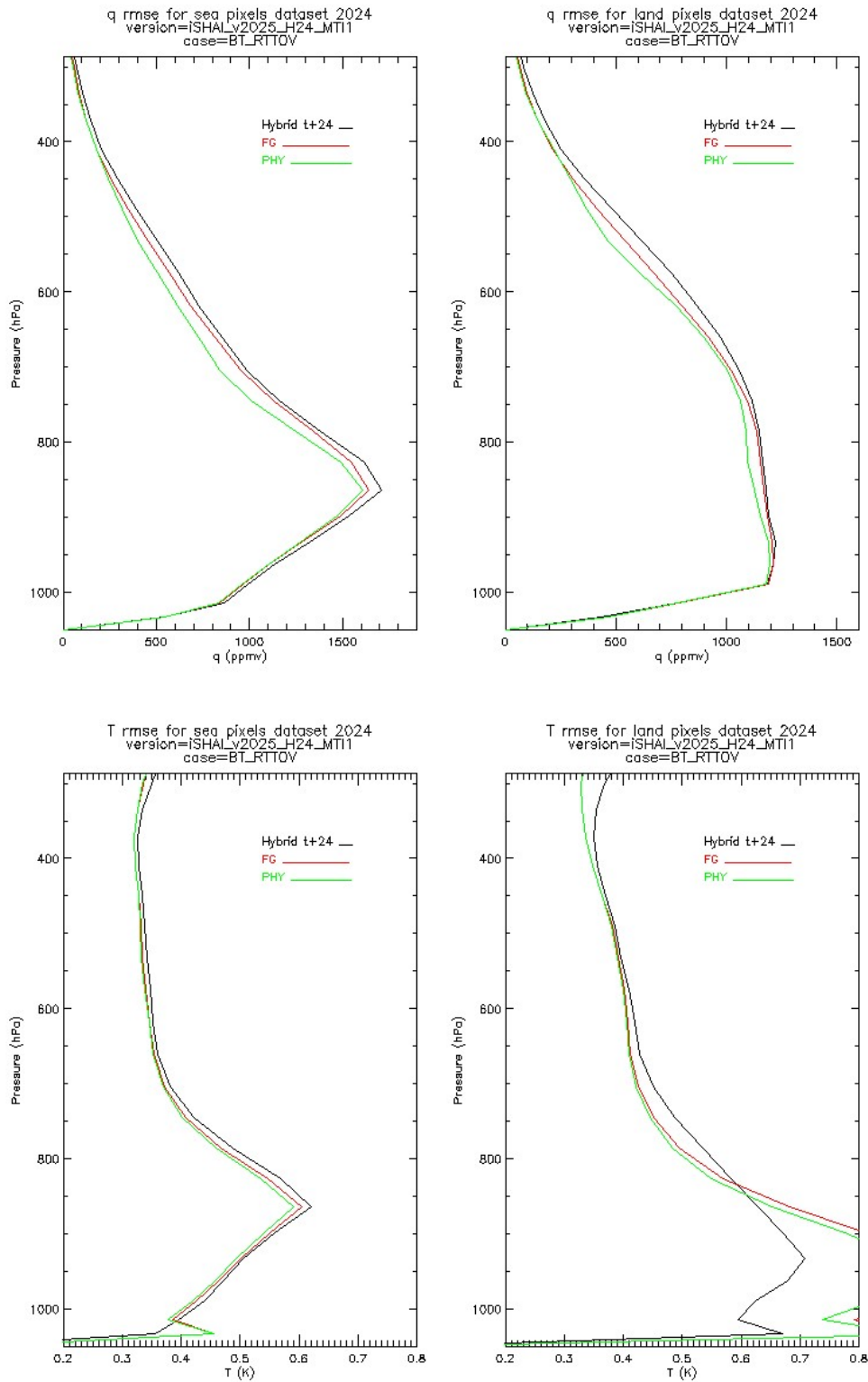


*Figure 30: **BT_RTTOV FCI MTI1 case:** RMSE profiles at different steps compared with ECMWF analysis (t+00) hybrid profiles. Top left) q RMSE on sea pixels, Top right) q RMSE on land pixels. Bottom left) T RMSE on sea pixels, Bottom right) T RMSE on land pixels.*

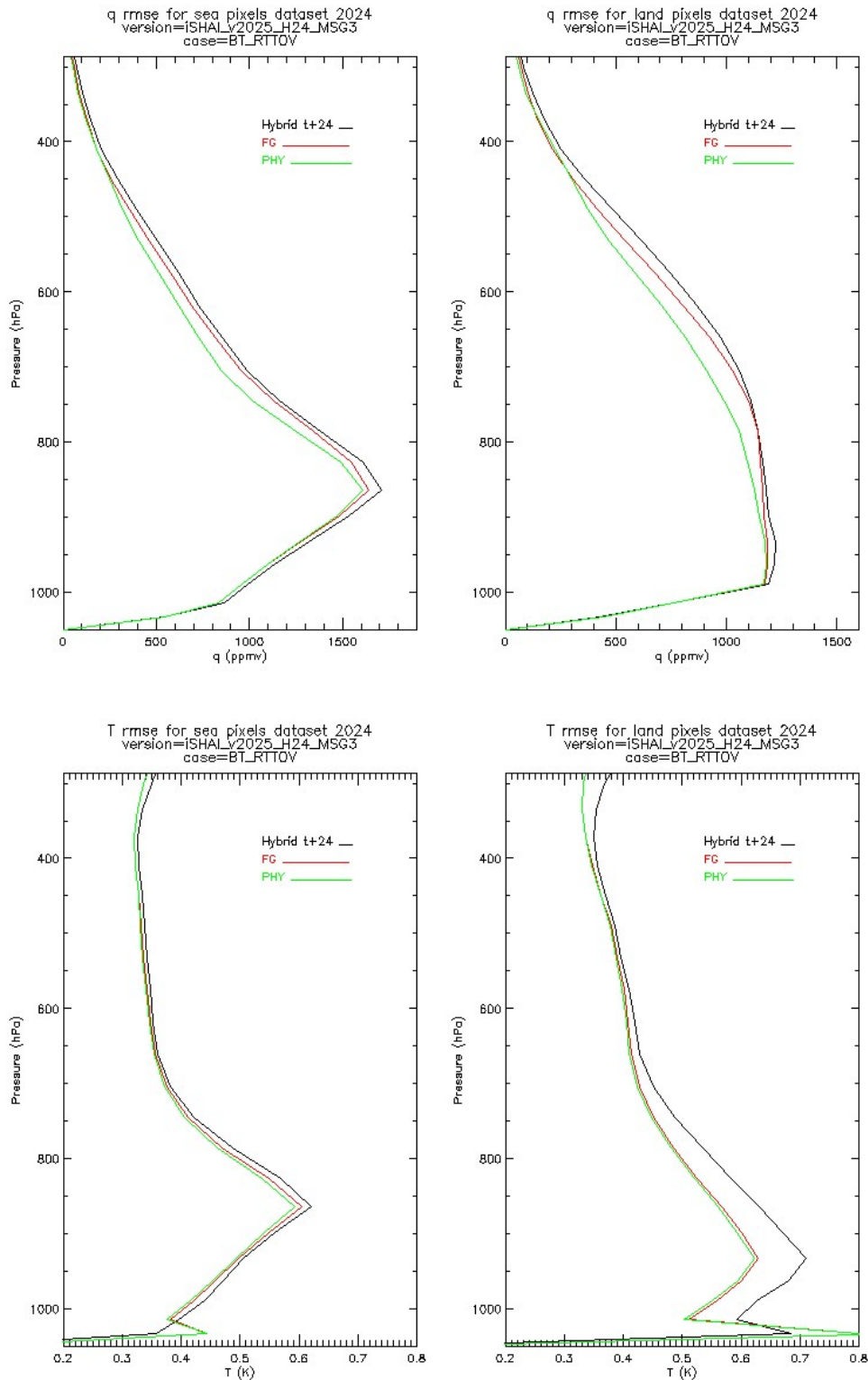


*Figure 31: **BT_RTTOV MSG3** case: RMSE profiles at different steps compared with ECMWF analysis (t+00) hybrid profiles. Top left) q RMSE on sea pixels, Top right) q RMSE on land pixels. Bottom left) T RMSE on sea pixels, Bottom right) T RMSE on land pixels.*

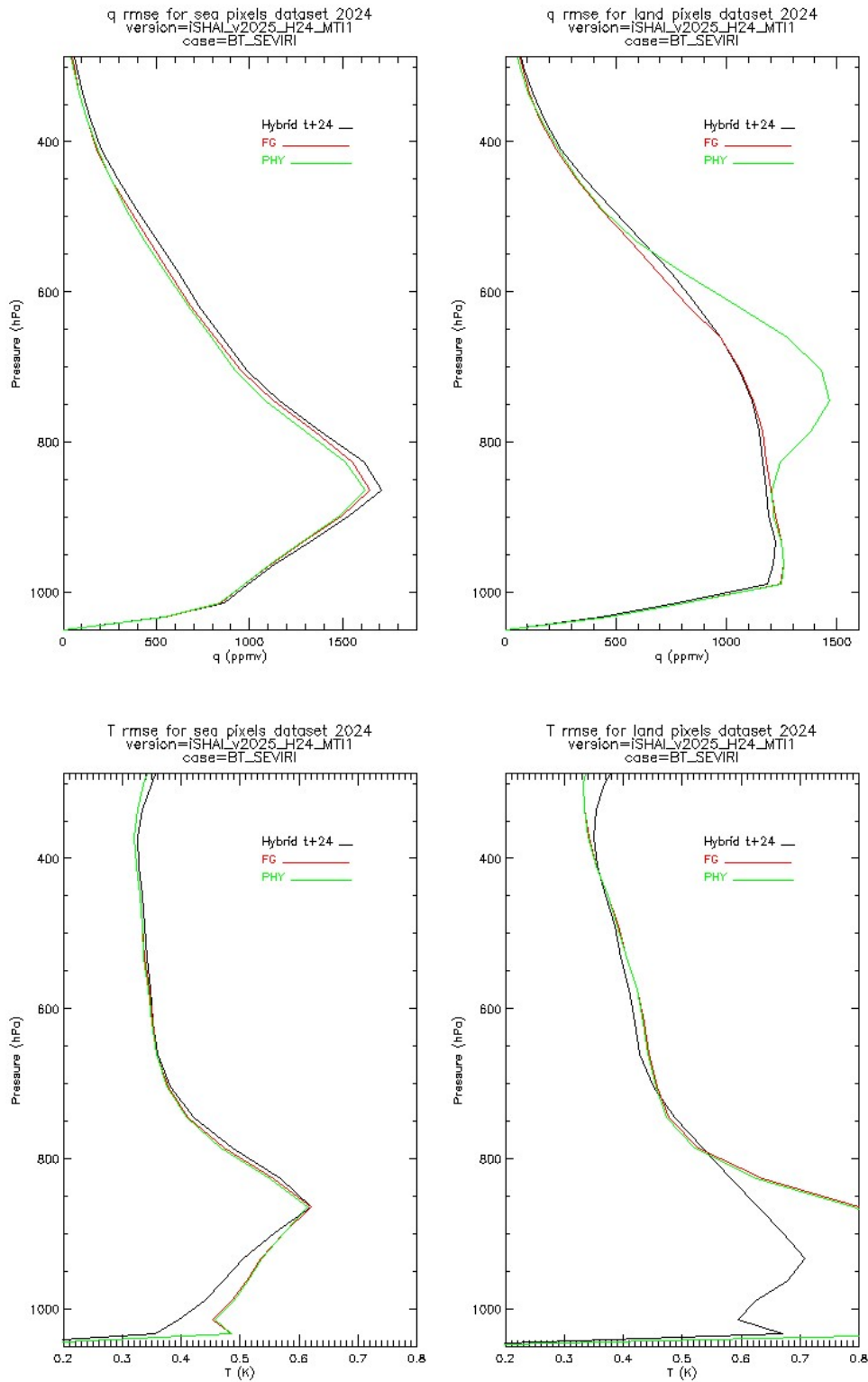


Figure 32: Real_BT FCI MTI case: RMSE profiles at different steps compared with ECMWF analysis (t+00) hybrid profiles. Top left) q RMSE on sea pixels, Top right) q RMSE on land pixels. Bottom left) T RMSE on sea pixels, Bottom right) T RMSE on land pixels.

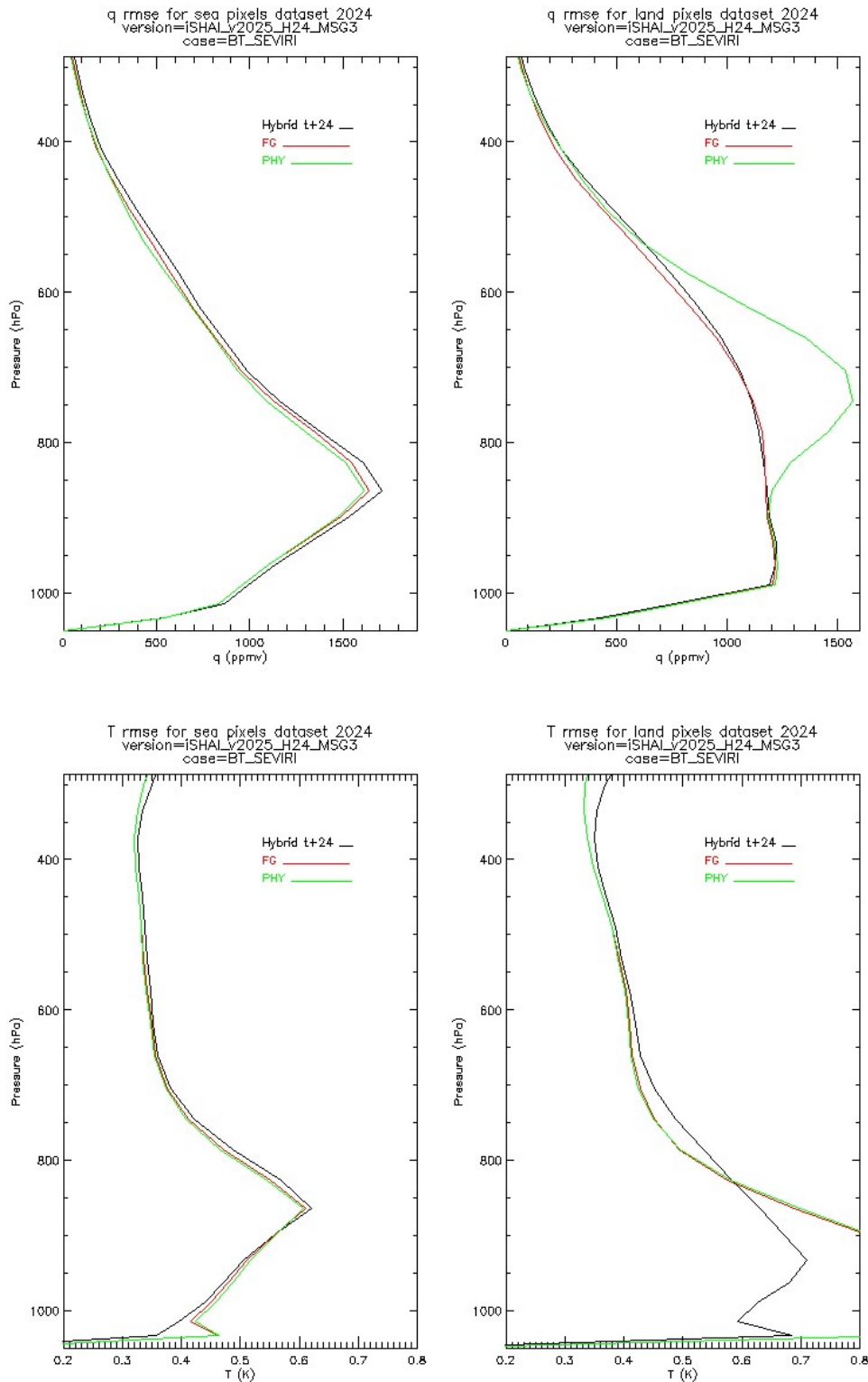


Figure 33: **Real_BT MSG3 case:** RMSE profiles at different steps compared with ECMWF analysis ($t+00$) hybrid profiles. Top left) q RMSE on sea pixels, Top right) q RMSE on land pixels. Bottom left) T RMSE on sea pixels, Bottom right) T RMSE on land pixels.

The FCI MTI1 T RMSE profiles is greater than the SEVIRI T RMSE profiles and it is likely due to the difference properties of FCI IR10.5 and FCI IR12.3 respect to SEVIRI IR10.8 and SEVIRI IR12.0. This early combined validation test FCI and MSG3 suggests the need to look for improvements in the iSHAI software that allow us to take advantage of the greater influence of the FCI IR10.5 compared to the SEVIRI IR10.8 one on T profile at low levels. The first modification

to test could be the incorporation as another parameter of the emissivity on FG regressions. In similar previous tests made with SEVIRI in the past it was discarded due to not get significant reduction and the generation of spatial discontinuities in region with strong gradient on emissivity (take into account the use on iSHAI of fixed emissivity atlases) on ML and HL layers. In CDOP-5 other test to do will be the study on the use of MTG-S/IRS emissivity atlases that could provide evolution, high quality and high spatial resolution on emissivity atlases.

3.5 VALIDATION OF GEO-iSHAI SKT: SKIN TEMPERATURE

In this Section the validation results of the Skin Temperature (SKT) are shown. This GEO-iSHAI output was introduced as a new output in release 2016. SKT is written just for nowcasting purposes and in order for the users to have access to this parameter. As an example, as SKT is used in the RTTOV calculations, the inspection of spatial gradients and temporal tendency could be used to detect the presence of non-adequately detected clouds or errors in the background NWP SKT.

The SKT should be taken as an indicative output and it should not be considered as SST or LST products because more controls and spatial and temporal tests would be needed. The SKT field of ECMWF has not a great quality especially over land pixels; due to this fact the spatial rmse in BT_SEVIRI case show great values over land. The result of the Figures in this SKT Section could be used to inform users of the discrepancies between the background NWP SKT and one optimal SKT in the pixels; but it must be taken into account that the discrepancies could be also due to physical reasons, due to undetected clouds or due to error in the emissivities, etc.

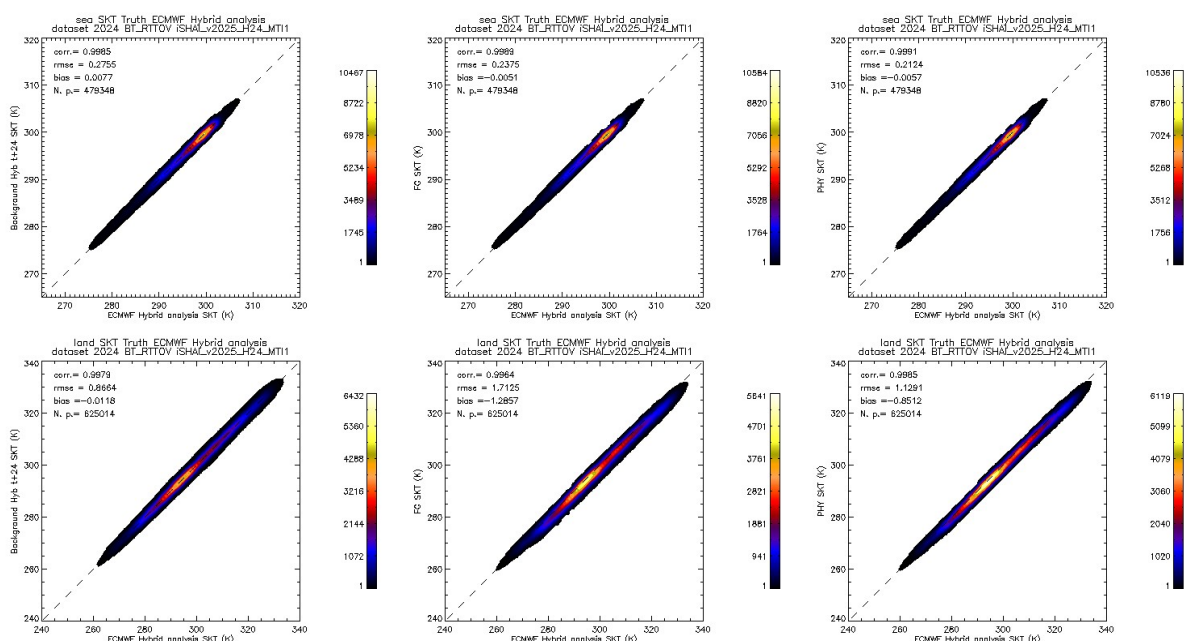


Figure 34: **BT_RTTOV FCI MT11 case: SKT 2D histograms.** (top) sea SKT. (bottom) land SKT. Left) SKT directly from background ECMWF hybrid GRIB (t+24), centre) SKT calculated after FG step profile, right) SKT calculated after physical retrieval step profile. In all case the ground truth is SKT from NWP-Hyb ECMWF analysis(t+00) profiles.

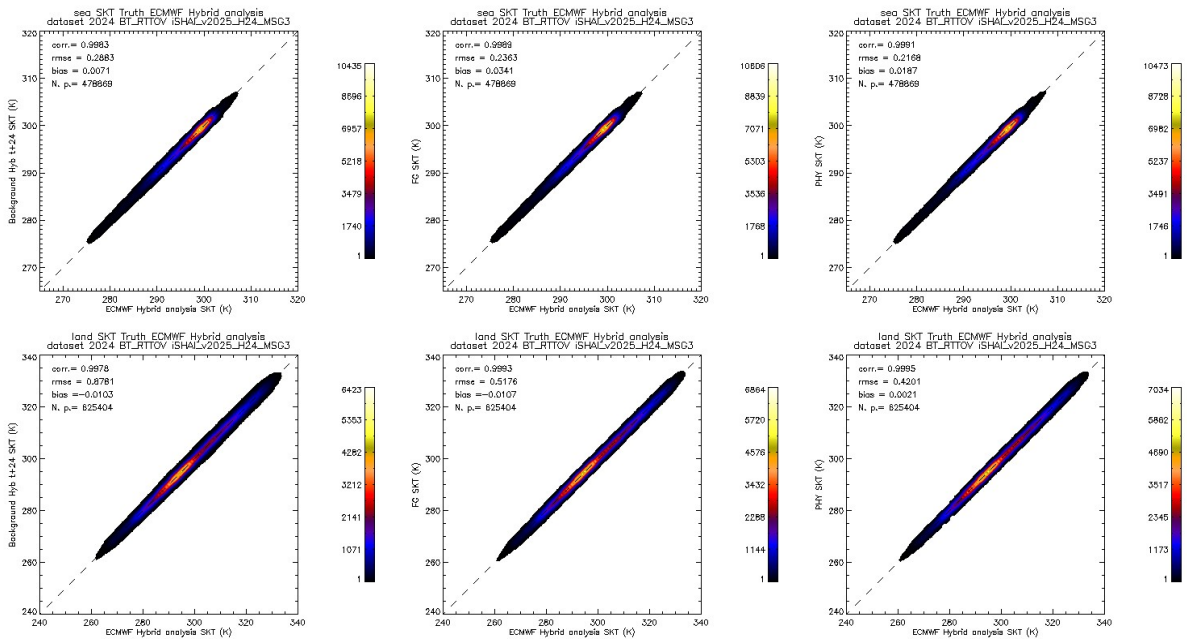


Figure 35: **BT_RTTOV MSG3** case: SKT 2D histograms. (top) sea SKT. (bottom) land SKT. Left) SKT directly from background ECMWF hybrid GRIB (t+24), centre) SKT calculated after FG step profile, right) SKT calculated after physical retrieval step profile. In all case the ground truth is SKT from NWP-Hyb ECMWF analysis(t+00) profiles.

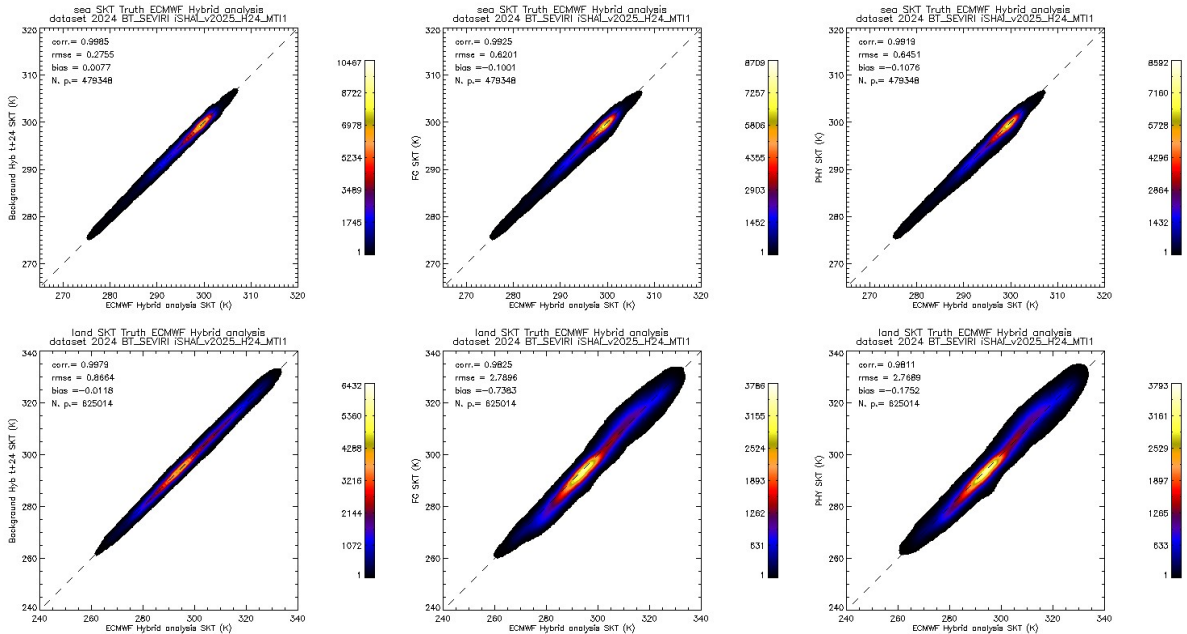


Figure 36: **Real_BT FCI MTI1** case: SKT 2D histograms. (top) sea SKT. (bottom) land SKT. Left) SKT directly from background ECMWF hybrid GRIB (t+24), centre) SKT calculated after FG step profile, right) SKT calculated after physical retrieval step profile. In all case the ground truth is SKT from NWP-Hyb ECMWF analysis(t+00) profiles.

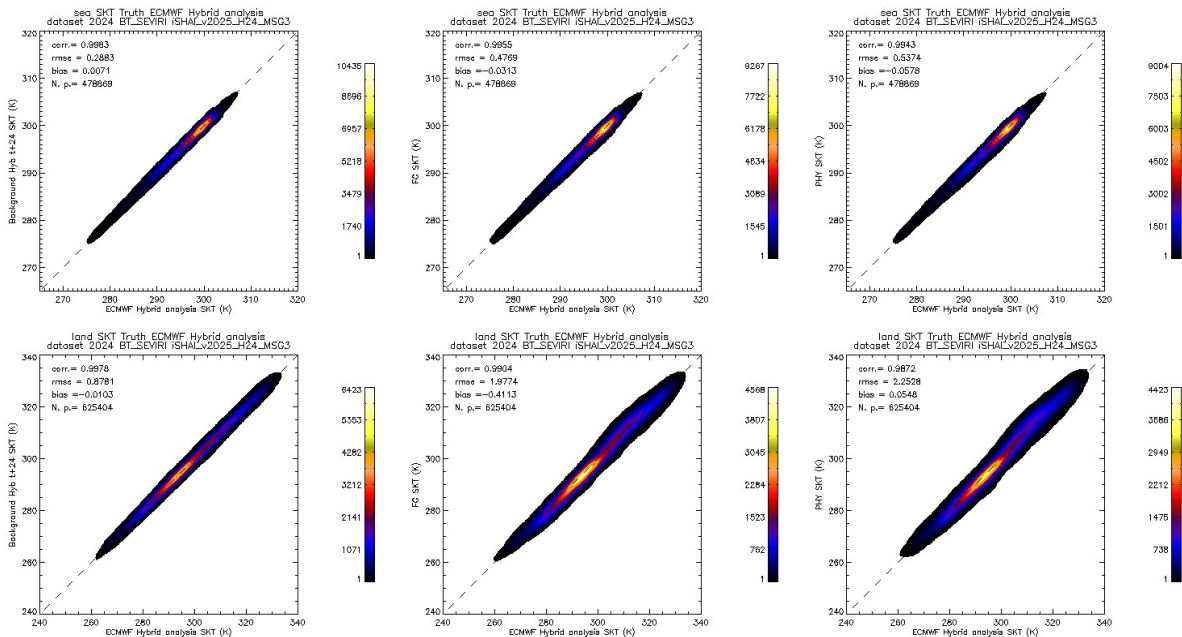


Figure 37: Real_BT MSG3 case: SKT 2D histograms. (top) sea SKT. (bottom) land SKT. Left) SKT directly from background ECMWF hybrid GRIB (t+24), centre) SKT calculated after FG step profile, right) SKT calculated after physical retrieval step profile. In all case the ground truth is SKT from NWP-Hyb ECMWF analysis (t+00) profiles.

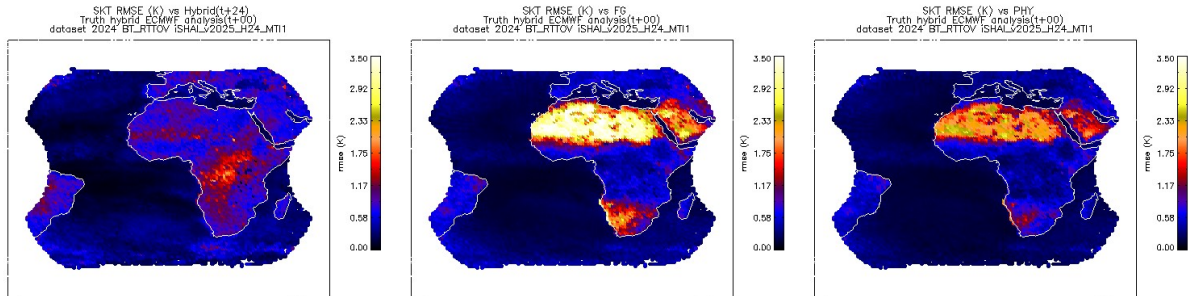


Figure 38: BT_RTTOV FCI MTI1 case: Spatial distribution of the SKT RMSE. (Left) SKT directly from background ECMWF hybrid GRIB (t+24), (centre) SKT calculated after FG non-linear regression step, (right) SKT calculated after physical retrieval step. In all case the ground truth are SKT from NWP-Hyb ECMWF analysis (t+00) profiles.

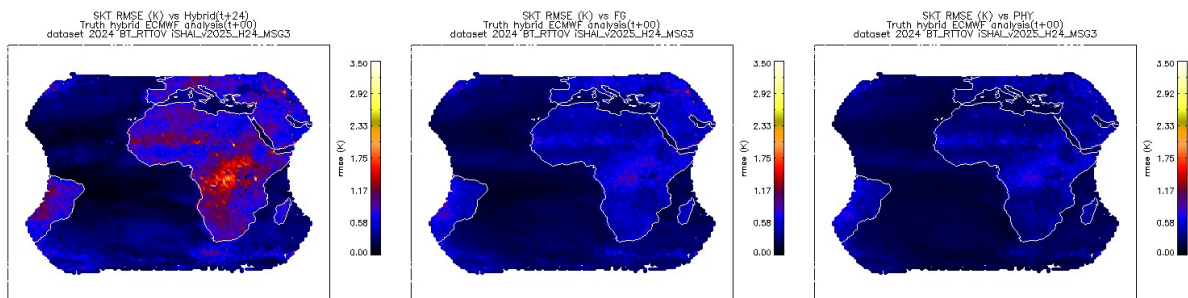


Figure 39: BT_RTTOV MSG3 case: Spatial distribution of the SKT RMSE. (Left) SKT directly from background ECMWF hybrid GRIB (t+24), (centre) SKT calculated after FG non-linear regression step, (right) SKT calculated after physical retrieval step. In all case the ground truth are SKT from NWP-Hyb ECMWF analysis (t+00) profiles.

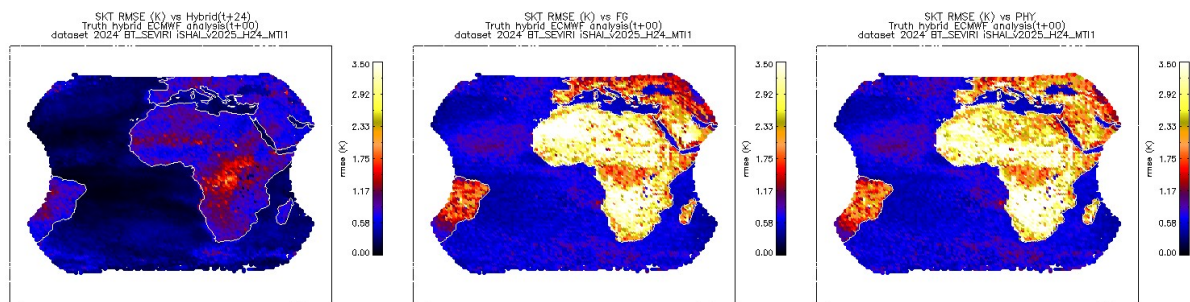


Figure 40: *Real_BT_FCI_MTI1* case: Spatial distribution of the SKT RMSE. (Left) SKT directly from background ECMWF hybrid GRIB (t+24), (centre) SKT calculated after FG non-linear regression step, (right) SKT calculated after physical retrieval step. In all case the ground truth are SKT from NWP-Hyb ECMWF analysis (t+00) profiles.

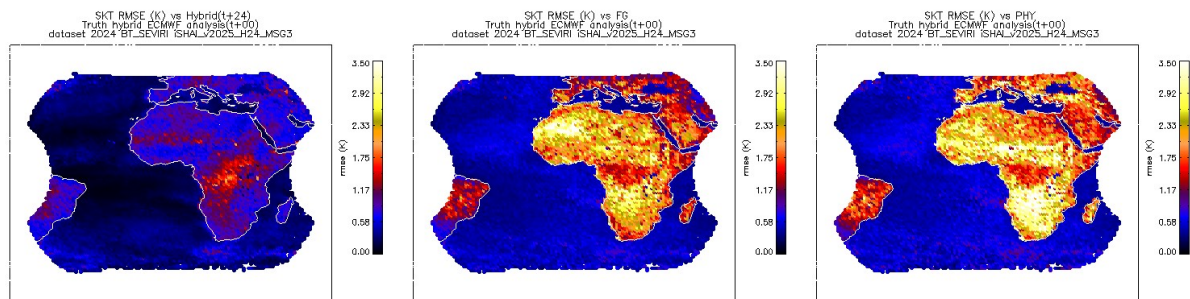


Figure 41: *Real_BT_MSG3* case: Spatial distribution of the SKT RMSE. (Left) SKT directly from background ECMWF hybrid GRIB (t+24), (centre) SKT calculated after FG non-linear regression step, (right) SKT calculated after physical retrieval step. In all case the ground truth are SKT from NWP-Hyb ECMWF analysis (t+00) profiles.

4. CONCLUSIONS

After this early validation of GEO-iSHAI with this limited period dataset, some provisional conclusions can be obtained:

- To build a good training and validation dataset is a very important and standing task for us. This continuous task has allowed the generation of a huge dataset. The use of this dataset has two main aims. The first one is to serve for the validation and tuning of the current version of the algorithm. The second one is the training, testing and validation of new versions of GEO-iSHAI. In the 2025 versions all the coefficients have been calculated from the GEO-iSHAI validation and training datasets (using ECMWF profiles).
- It is needed to improve the process for screening of cloud contaminated pixels. As can be shown in the Figures corresponding to Real_BT cases there are still cloudy contaminated pixels that increase the rmse values on the case of real FCI or SEVIRI tests.
- The GEO-iSHAI processor with coefficients trained using the ECMWF NWP Hybrid dataset, allowing the use of ECMWF GRIB files on hybrid levels, improves strongly the performance over the regular version of the GEO-iSHAI, which uses ECMWF NWP fixed pressure fields. For the users that use ECMWF to feed NWC SAF software in real time, it is strongly recommend to make the effort of downloading from the MARS the ECMWF GRIB files on hybrid levels and to use the GEO-iSHAI HYB mode. For the users that use their own NWP models to feed NWC SAF software in real time, it is strongly recommended they make the effort to provide optimal vertical resolution to GEO-iSHAI.
- The performance of the regular GEO iSHAI versions 2025 with fixed pressure NWP input will tend to be similar than the one for the GEO-iSHAI hybrid mode if the number of available fixed pressure vertical levels increases. Then, it is strongly recommend to the users to feed to the regular GEO iSHAI inputs with the highest available number of fixed pressure levels.
- It is also recommended to feed the GEO-iSHAI with the highest possible temporal and spatial resolution.
- Validation has been performed for near the complete FCI or SEVIRI disc. It will be used a slightly wider region in next validation activities. Due to memory issues and in order to speed-up the process executing at the same time FCI and SEVIRI chains it has not executed at the full disk.
- Best results are obtained for humidity in medium layers due to the contribution of the water vapour channels. In this layer the GEO-iSHAI improves the information beyond the background NWP on the humidity profile.
- GEO imager satellites has limited information to improve the vertical information beyond the forecast, but it does provide useful spatial and temporal information. This limitation is clear for the vertical information of temperature and stability indices.
- The performances and RMSE of the GEO iSHAI parameters from FCI and MSG are similar and all the parameters are better than is requested in the Product Requirement Document [AD.4]
- A good BT bias correction is essential for GEO-iSHAI. A mechanism to calculate and distribute frequently and updated SEVIRI BT bias correction has been implemented through a web page in the NWC SAF web, to provide frequent and rapid updates of the SEVIRI BT bias correction. A similar mechanism was developed for AHI and ABI and they are available on <http://www.nwcsaf.org/web/guest/bias-bt-correction-coefficients>. It will be available for FCI, SEVIRI, AHI and ABI with version 2025 when version 2025 be distributed.
- Validation has been performed for an initial period when FCI started to be available but it would be needed to repeat for a complete year.
- This reduction of RMSE is lower using real bias corrected FCI or SEVIRI BTs due to noise of the satellite, errors in radiative transfer models and bias correction, lack of good emissivity

atlases, etc and the lack of a real truth. But the algorithm is sensible to discrepancy between synthetic and real FCI or SEVIRI BTs and then is able to advice the users of any discrepancy in the forecast NWP used as background NWP; it is recommend the use of the parameters with the differences between the NWP used as input to GEO iSHAI and the retrieved profiles in order to detect any discrepancy between the forecast model and the real observations of the FCI or SEVIRI images.

- In previous Validation Reports the initial validation of AHI and ABI in synthetic RTTOV case over SEVIRI 2017 training and validation dataset shown that the performance is slightly better due to the addition of two channels. For a better improvement of iSHAI products it will be needed to wait to MTG-IRS era. The generalization of the validation process from FCI or SEVIRI to AHI and ABI will be used in next future to generalize the validation of MTG-FCI to MTG-IRS.